UNITED NATIONS EDUCATIONAL, SCIENTIFIC AND CULTURAL ORGANIZATION
INTERNATIONAL CENTRE FOR THEORETICAL PHYSICS
I.C.T.P., P.O. BOX 586, 34100 TRIESTE, ITALY, CABLE: **CENTRATOM TRIESTE**

SMR/697-7

RESEARCH WORKSHOP ON CONDENSED MATTER PHYSICS
(21 June - 3 September 1993)

WORKING PARTY ON SMALL SEMICONDUCTOR STRUCTURES
(2 - 13 August 1993)

" ELECTRONIC STRUCTURE OF SEMICONDUCTOR SUPERLATTICES "

M. KRIECHBAUM
Inst. Theoret. Physik, Univ. Graz
Universitätspl.5
A - 8010 Graz
Austria

These are preliminary lecture notes, intended only for distribution to participants

ELECTRONIC STRUCTURE

Quantised Semiconductor Systems

Semiconductor Superlattices
Quantum Wells

M. Kriechbaum
Inst. Theoret. Physik, Univ. Graz
Universitätspl. 5
A-8010 Graz, Austria

G. Bauer, Univ. Linz

H. Pascher, Univ. Bayreuth

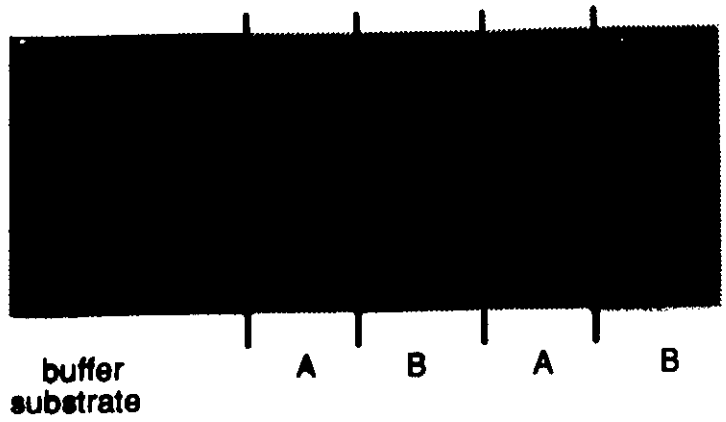

Band-offset at interface
models, first principles

energy dispersion
$E(k_X, k_y, k_Z)$,
$E(B, k_B, z_C)$
Faraday (B_{perp}), Voigt (B_{inpl}) configuration

Strain Effects

optical properties
absorption constant

Photo-magnetisation of magnetic impurities

Electrostatic potential due to charge transfer

Excitons

Impurities

resonant tunnelling

Envelope Function Approximation,
Empirical Tight Binding

Band Offsets in Semiconductor Heterojunctions
E.T.Yu, J.O.McCaldin, and T.C.McGill
Solid State Physics **46**,2 1992

Semiconductors and Semimetals
R.K.Willardson and A.C.Beer, eds.
last volumes

G. Bastard: Wave Mechanics applied to
Semiconductor Heterostructures
Les Editiones de Physique 1988

Claude Weissbuch and B. Vinter
Quantum Semiconductor Structures
Academic Press 1991

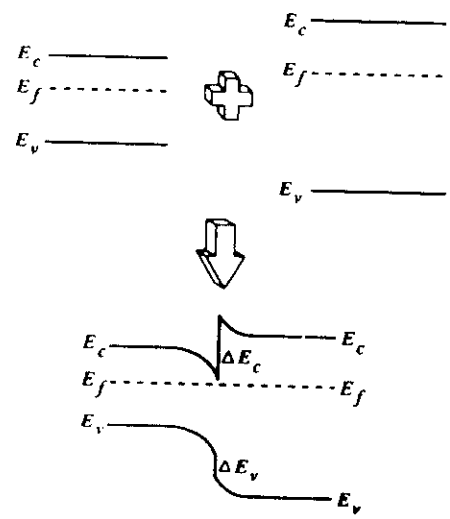

FIG. 1. Conduction- and valence-band offsets in a semiconductor heterojunction. E_c and E_v are the conduction- and valence-band edges, respectively, and E_f is the Fermi level. The band offsets ΔE_c and ΔE_v are abrupt discontinuities in the band edges at the heterojunction interface. Electrostatic band bending also occurs because of charge redistribution near the heterojunction interface.

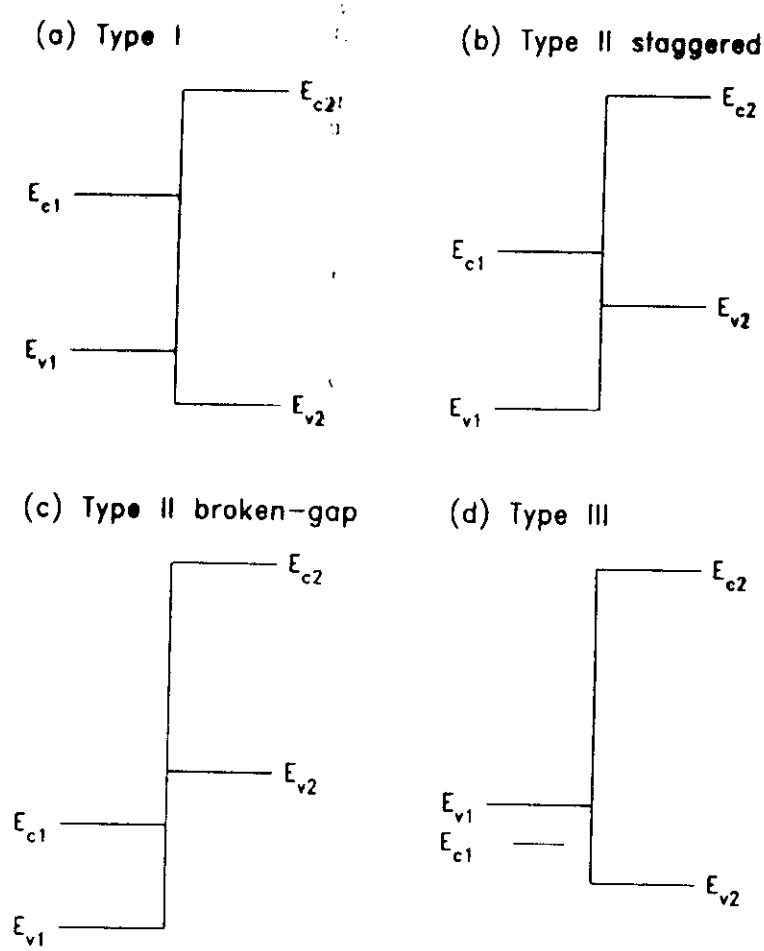

FIG. 2. Possible types of band alignments at a semiconductor interface. Conduction- and valence-band-edge positions for each material have been labeled E_c and E_v, respectively, with the shaded regions indicating the energy band gap in each material.

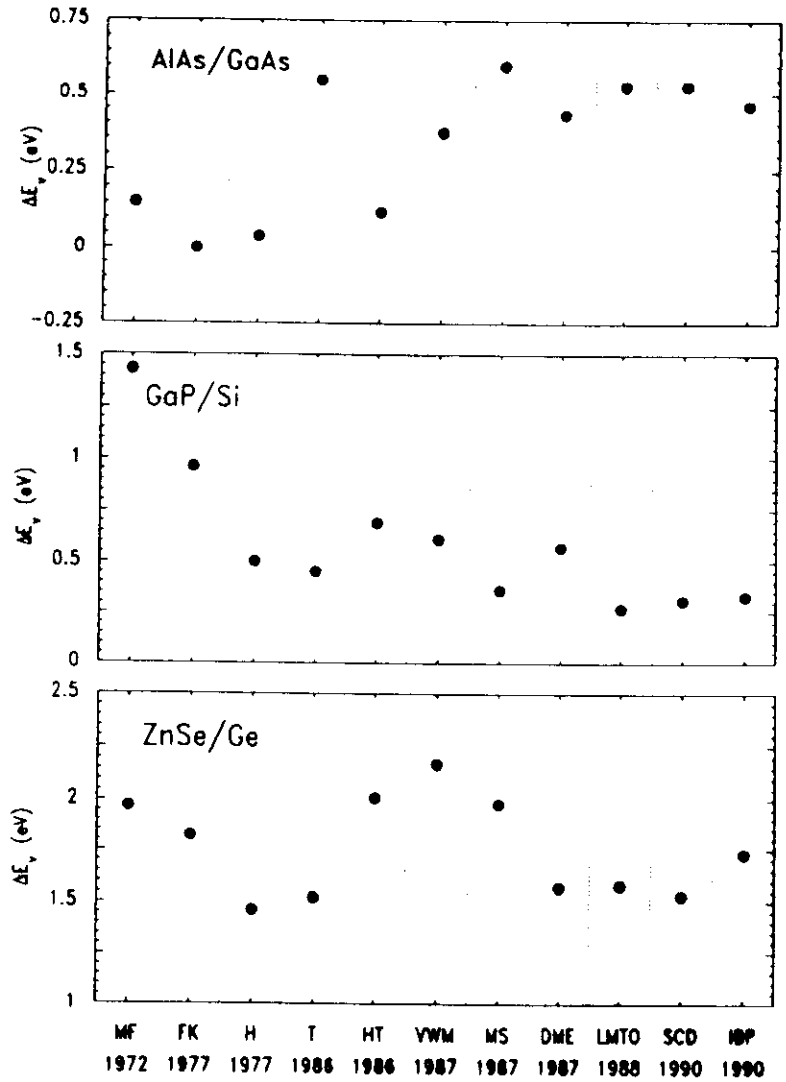

FIG. 11. A comparison of theoretical and experimental band offset values for the AlAs/GaAs, GaP/Si, and ZnSe/Ge heterojunctions. Different theories are plotted in approximately chronological order, and the range of experimental values thought to have been valid at the time each theory was developed has been shaded. For extensively studied systems such as AlAs/GaAs, recent theories agree well with experiment. Agreement between theory and experiment, and even among theoretical values, is poorer for less studied systems such as GaP/Si and ZnSe/Ge. Theoretical predictions are from the following sources; MF 1972, Ref. 71; FK 1977, Ref. 23; H 1977, Ref. 24; T 1986, Ref. 28; HT 1986, Ref. 29; VWM 1987, Ref. 84; MS 1987, Ref. 84; DME 1987, Ref. 39; LMTO 1988, Ref. 40; SCD 1990, Ref. 43; IBP 1990, Ref. 87.

Flores, Tejedor, Tersoff

The interface induces gap states, different hights on both sides of the interface lead to interface dipoles, electrostatic screening reduces the potential step V to V/ε, thus band alignment at Effective midgap point

$$G(\vec{R},E)=\int d^3r\sum_{nk}\frac{\Psi^*_{nk}(\vec{r})\Psi_{nk}(\vec{r}+\vec{R})}{E-E_{nk}}=\sum_{nk}\frac{e^{i\vec{k}\cdot\vec{R}}}{E-E_{nk}}$$

R lattice vector perpendicular to interface define midgap point E_B related to Kohn branchpoint in one dimension where conduction and valence band contribute equally to G calculation with LAPW, rigid shift of conduction band

Cardona Christensen

Dielectric midgap energy average of upper valence and lower conduction band

Christensen

Self consistent relativistic linear-muffin-tin-orbital method in supercell geometry Cation d-states hybridize with valence band maximum and influence offset

Lambrecht Segall Andersen

Superlattice geometry with linear-muffin-tin-orbital method. Correct band alignment is obtained by minimizing the total energy with respect to a *single* parameter: the interface dipole

Band Offset: A Supercell Calculation

(C.G.Van der Walle and R.M.Martin,
Phys.Rev. **35**, 8154 1987)

first principle calculation the band offset at a semiconductor interface A/B

superlattice geometry, based on local-density-functional theory and non-local norm conserving *ab initio* pseudopotentials

Spin-orbit splitting effects in the valence band were added *a posteriori*

III-V and II-VI semiconductors

transitivity rule:

$$\Delta E_c^{A/B} + \Delta E_c^{B/C} + \Delta E_c^{C/A} = 0$$

$$E_{total} = T + V + \int E_{xc}(\mathbf{r})\mathrm{d}^3 r,$$

$$T = \sum_i \psi_i^*(\mathbf{r})\left(-\nabla^2/2m\right)\psi_i(\mathbf{r})\mathrm{d}^3 r,$$

$$V = \sum_{i\mu l} \int \psi_i^*(\mathbf{r}) U_{\mu l}\left(\mathbf{r} - \mathbf{R}_\mu\right)\hat{P}_l \psi_i(\mathbf{r})\mathrm{d}^3 r$$

$$+ \tfrac{1}{2}\iint \frac{2\rho(\mathbf{r})\rho(\mathbf{r}')}{|\mathbf{r} - \mathbf{r}'|}\mathrm{d}^3 r\,\mathrm{d}^3 r' + \sum_{\mu \neq \nu} \frac{Z^2}{|\mathbf{R}_\mu - \mathbf{R}_\nu|}$$

$$\rho(\mathbf{r}) \equiv \sum_i |\psi_i(\mathbf{r})|^2$$

$$\left(-\frac{\nabla^2}{2m} + \sum_{\mu l} U_{\mu l}\left(\mathbf{r} - \mathbf{R}_\mu\right)\hat{P}_l + \int \frac{2\rho(\mathbf{r}')}{|\mathbf{r} - \mathbf{r}'|}\mathrm{d}^3 r' + \mu_{xc}(\mathbf{r})\right)\psi_i(\mathbf{r})$$

$$\equiv \varepsilon_i \psi_i(\mathbf{r})$$

$$\mu_{xc}(\mathbf{r}) \equiv \partial E_{xc}(\mathbf{r})/\partial\rho(\mathbf{r})$$

$$\mu_{xc}(\mathbf{r}) \propto \sqrt[3]{\rho(\mathbf{r})}$$

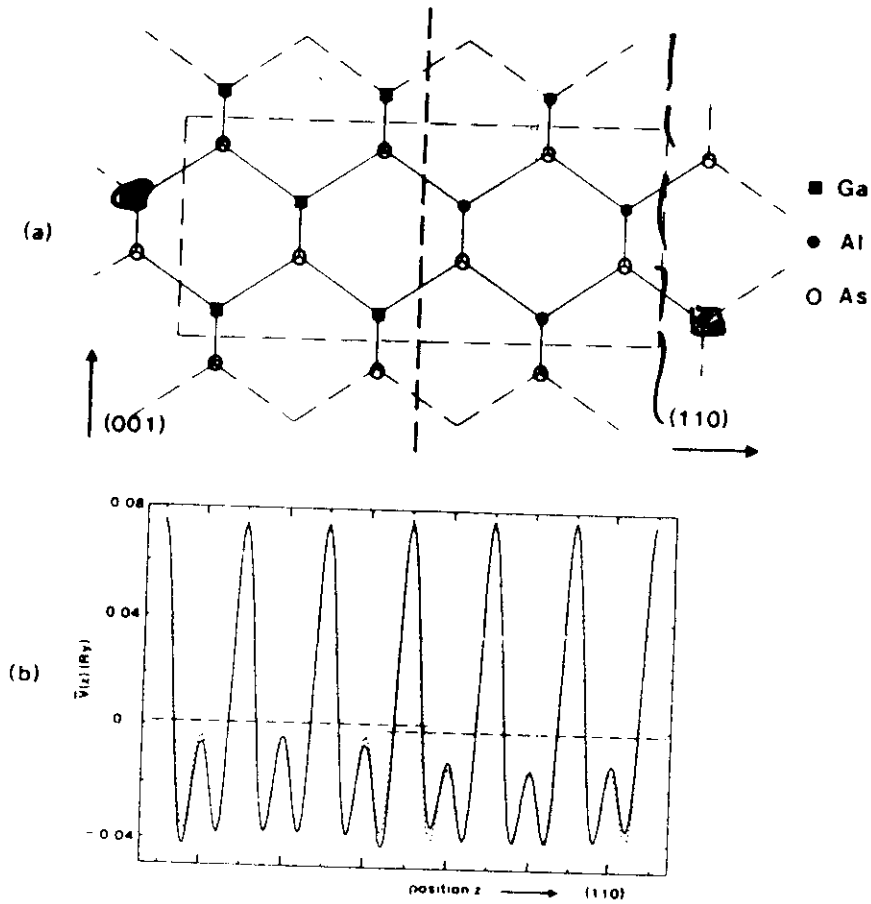

FIG. 1. (a) Schematic representation of a GaAs/AlAs (110) interface. The supercell used in the interface calculations is indicated in dotted lines; it contains 12 atoms and 2 identical interfaces. (b) Variation of the $l=1$ component of the total potential $\bar{V}(z)$ [as defined in Eq. (1)] across the (110) interface. The dashed lines represent the corresponding potentials for the bulk materials. These coincide with $\bar{V}(z)$ in the regions far from the interfaces. However, the average levels of the two bulk potentials (dashed horizontal lines) are shifted with respect to one another.

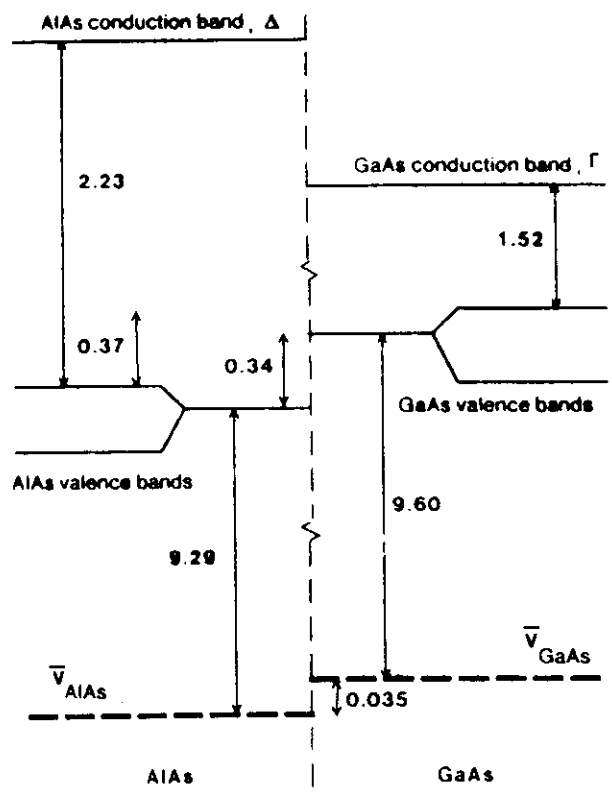

FIG. 2. Derivation of band lineups: relative position of the average potentials $\overline{V}_{AlAs}$ and $\overline{V}_{GaAs}$, and of the AlAs and GaAs valence and conduction bands. All values shown are derived with the $l=1$ angular momentum component chosen as the reference potential; the band lineups, however, are unique and independent of this choice. Valence-band splittings due to spin-orbit splitting are indicated separately. Experimental band gaps were used to derive conduction-band positions.

Band Offset: An Empirical Tight Binding Model

(M. Kriechbaum, P.Kocevar, H.Pascher and G.Bauer,
IEEE J. Quant El. **24**, 1727, 1988)

(J. C. Slater and G. F. Koster, Phys Rev **94**, 1498, 1954)

$$\Psi_{\mathbf{k}}(\mathbf{r}) = \frac{1}{\sqrt{N}} \sum_{njm\rho} A_{\mathbf{k}njm\rho} \sum_{\mathbf{R}} \Phi_{njm}(\mathbf{r} - \mathbf{R} - \rho) \exp(i\mathbf{k} \cdot (\mathbf{R} + \rho))$$

Löwdin functions Φ

$$\langle \Phi(\mathbf{r} - \mathbf{R} - \rho) | \Phi(\mathbf{r} - \mathbf{S} - \sigma) \rangle \propto \delta_{RS\rho\sigma}$$

$$H\Psi_{\mathbf{k}} = \left(-\frac{\nabla^2}{2m} + V(\mathbf{r}) + V_{spin-orbit} \right) \Psi_{\mathbf{k}} = E\Psi_{\mathbf{k}}$$

$$V(\mathbf{r}) = \sum_{\mathbf{R},\rho} v_{\rho}(\mathbf{r} - \mathbf{R} - \rho)$$

$$\sum_{b} (H_{\mathbf{k},ab} - E_{\mathbf{k}}) A_b = 0$$

$$H_{\mathbf{k},(njm\rho)^a(njm\rho)^b} = \left\langle \sum_{\mathbf{R}a} \Phi_a(\mathbf{r} - \mathbf{R} - \rho_a) \middle| H_{\mathbf{k}} \middle| \sum_{\mathbf{S}b} \Phi_b(\mathbf{r} - \mathbf{S} - \rho_b) \right\rangle$$

STRUCTURE OF IV - VI COMPOUNDS

CUBIC

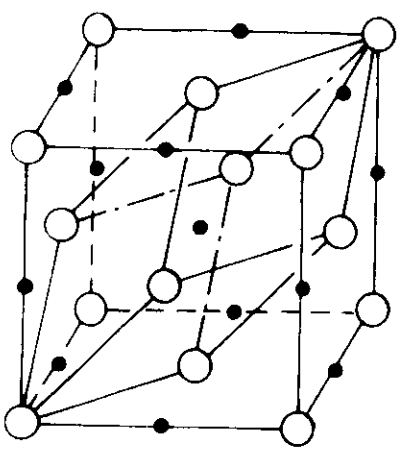

RHOMBOHEDRAL

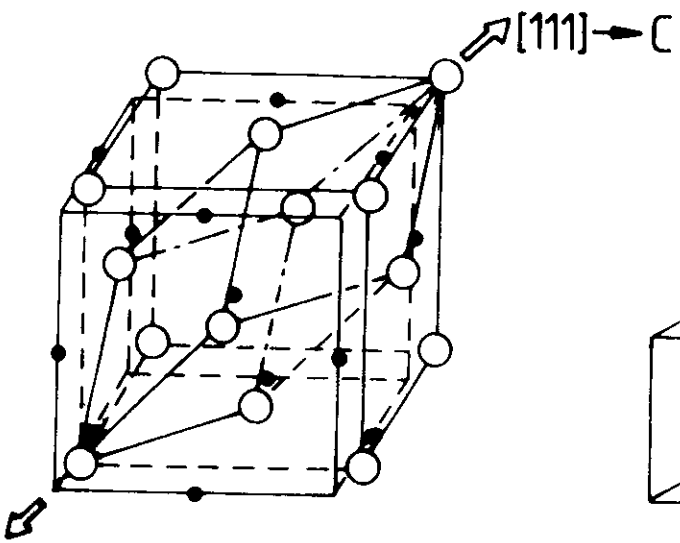

ORTHORHOMBIC

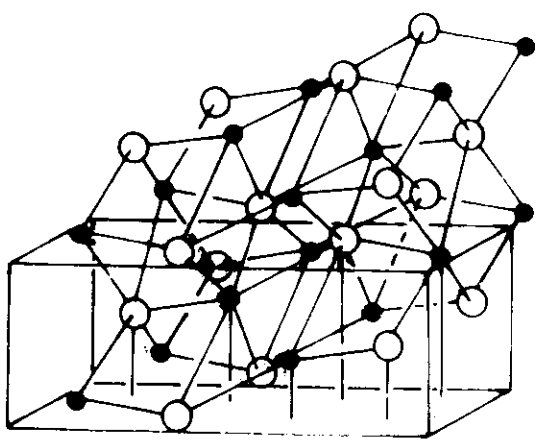

Lead chalcogenides: rock-salt structure

PbTe/SnTe

	K	L	M	N	O	P
Pb82	2	8	18	32	18	s^2p^2
Sn50	2	8	18	s^2p^2		
Te52	2	8	18	18	s^2p^4	

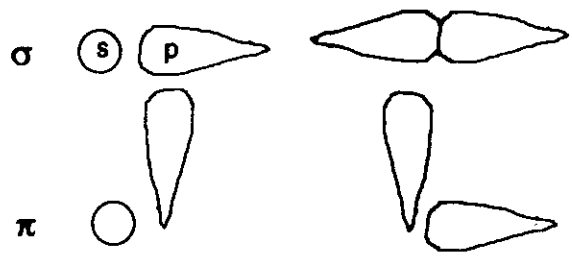

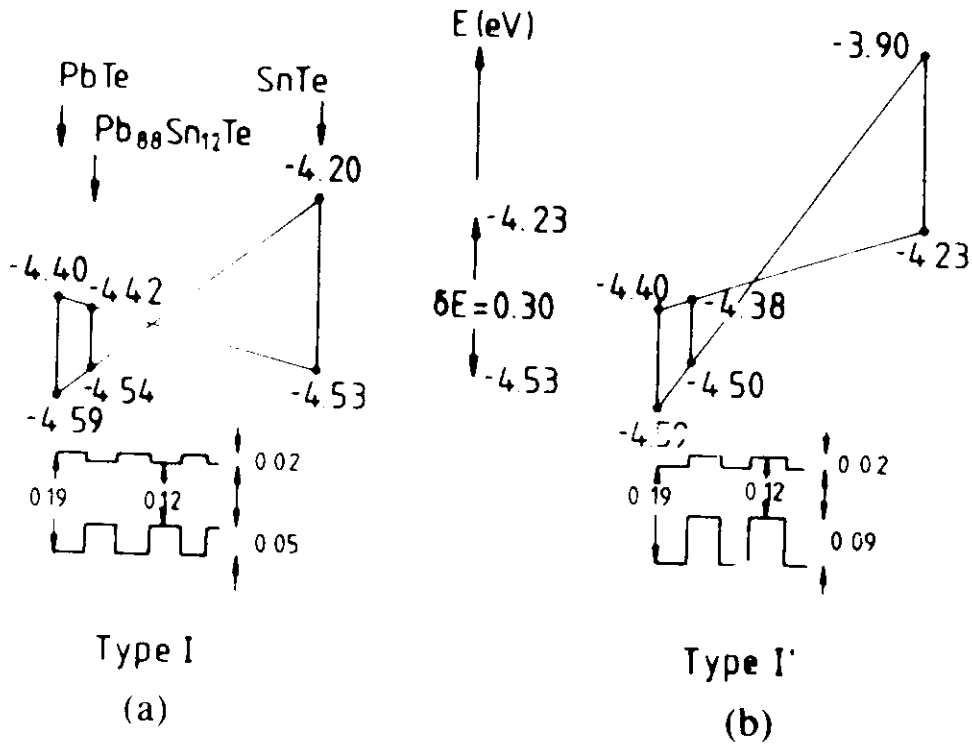

Fig. 4. Relative band ordering in PbTe/SnTe superlattices. (a) Present ETB result. (b) Equivalent type I′ ordering.

Charge exchange:

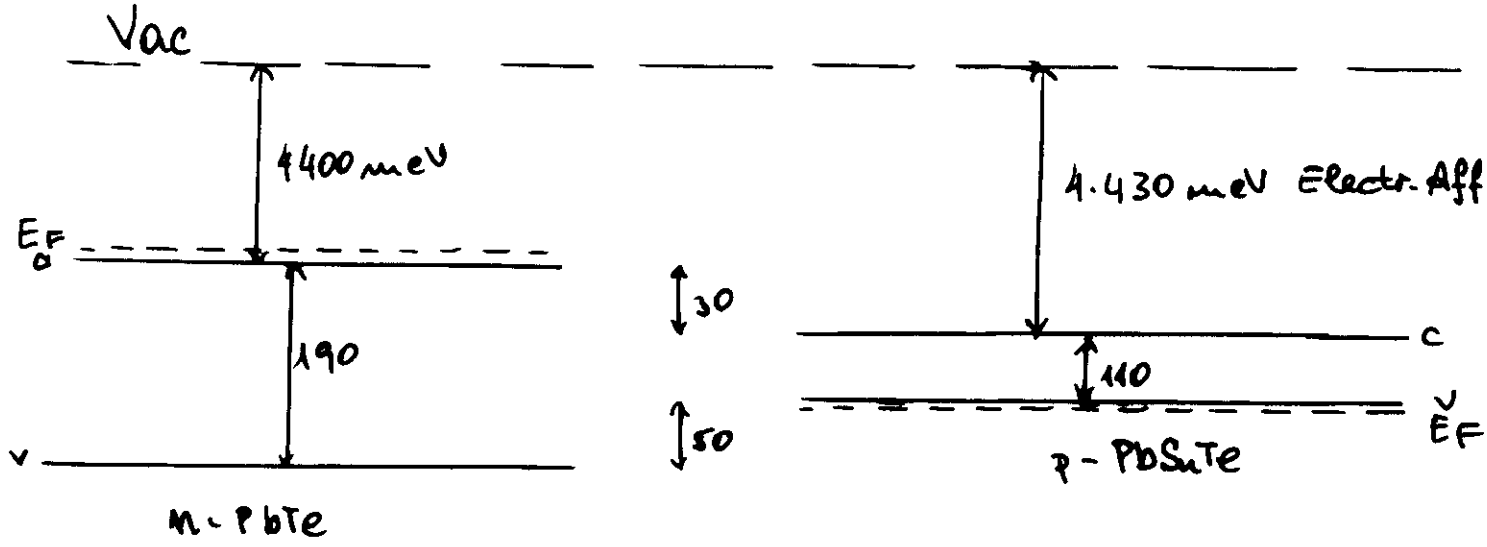

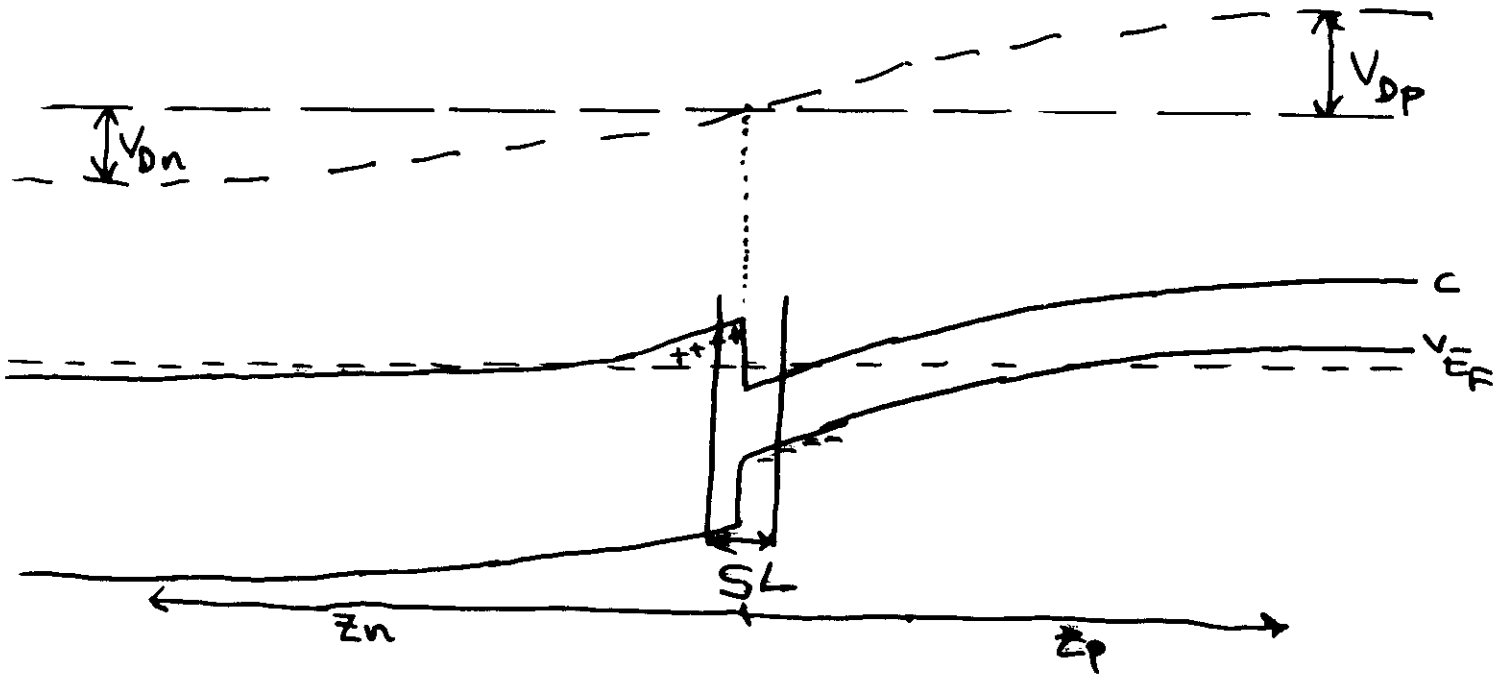

depletion length

$$z = \sqrt{\frac{2 V_D \epsilon}{N}} \quad , \quad V_{D_p} + V_{D_n} = E_{F_p} - E_{F_n} \quad , \quad N_A z_p = N_D z_n$$

$N_A = 4 \times 10^{17}\ cm^{-3}$
$N_D = 2 \times 10^{17}\ cm^{-3}$
$\epsilon_{PbSnTe} = 2500$
$\epsilon_{PbTe} = 1300$

$V_{Dn} = 135$ meV
$V_{Dp} = 35$ meV
$x_n = 311$ nm
$x_p = 155$ nm

Envelope Function Approximation

$$\left\{\begin{array}{l}\dfrac{p^2}{2m}+V(\vec{r})+U(\vec{r})+ \\ \qquad \dfrac{\hbar^2}{4m^2c^2}\vec{\sigma}\cdot\left[(\nabla V+\nabla U)\times\vec{p}\right]+ \\ \qquad\quad g\mu_B\vec{\sigma}\cdot\vec{B}\end{array}\right\}\Psi(\vec{r})=E\Psi(\vec{r})$$

$$\vec{p}=\frac{\hbar}{i}\nabla+\frac{e}{c}\vec{A}$$

$$\vec{B}=\nabla\times\vec{A}$$

$$V\left(\vec{r}+\vec{R}\right)=V(\vec{r})$$

Coulomb interactions among the electrons are included to some extent (e.g. Slater exchange or LDA) in the one electron potential V(r)

absence of a magnetic field and for a perfect crystal (U=0) due to the periodicity of V(r) characterised by a vector $\vec{k}$ in the reciprocal vector space

assume that all solutions $u_{nk_0}(\vec{r})$ of the Schrödinger equation for a perfect crystal are known for a particular value $\vec{k}_0$

$$\Psi(\vec{r}) = \sum_n f_n(\vec{r}) u_{nk_0}(\vec{r})$$

For sufficiently weak perturbations U(r) or small magnetic fields or also k values sufficiently close to k_0 the envelope functions will be almost constant on the scale of the lattice periodicity R on which the functions u are rapidly oscillating

$$\int d^3r\, u_{n'}^*(\vec{r})[H-E]\Psi(\vec{r}) =$$
$$\int d^3r\, u_{n'}^*[H-E]\sum_n f_n u_n$$

$$\sum_n \left\{ \left(E_n - E + \frac{p^2}{2m} + U \right)\delta_{n'n} + \vec{P}_{n'n}\cdot\vec{p} + \frac{\hbar^2}{4m^2c^2}\vec{\sigma}\cdot[\nabla U \times \vec{p}] \right\} f_n = 0,$$
$$n' = 1,2,3,\ldots$$

$$\vec{P}_{n'n} = \int_\Omega d^3r\, u_{n'k_0}^* \left(\frac{\hbar}{im}\nabla + \frac{\hbar^2}{4m^2c^2}\nabla V \times \sigma \right) u_{nk_0}$$

in semiconductors only few bands lye close to the bands comprising the fundamental gap

$$f_n = -\frac{1}{E_n - E}\sum_{n' \le N}\left\{\vec{P}_{nn'}\cdot\vec{p} + \text{spin orbit}\right\}f_{n'}$$

$$\sum_{n'=1}^{N}\left\{\begin{array}{l}(E_n - E)\delta_{nn'} + \\ \quad\left(\vec{P}_{nn'} + \dfrac{\hbar^2}{4m^2c^2}\nabla U\times\sigma\right)\cdot\vec{p} + \\ \qquad\qquad \vec{p}Q_{nn'}\vec{p} + g\mu_B\sigma\cdot\vec{B}\end{array}\right\}f_{n'} = 0,$$

$n = 1,\ldots N$

the momentum matrix elements P and the far band contributions Q obey the symmetry requirements of the group of the wave vector b_{k_0}

zinc blende: Γ point (k_0=0)

$\mathcal{D}_{k_0}$ is the improper tetraeder group:

$$H = \begin{bmatrix} H^{66} & H^{68} & H^{67} \\ H^{86} & H^{88} & H^{87} \\ H^{76} & H^{78} & H^{77} \end{bmatrix}$$

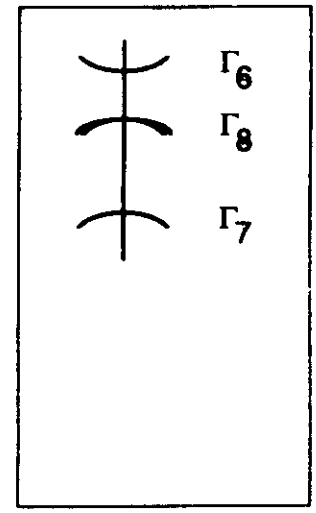

$$H^{88} = E_g + \frac{\hbar^2}{m} \times$$

$$\begin{bmatrix} -\frac{\gamma_1+\gamma_2}{2}(x^2+y^2) + \left(\gamma_2 - \frac{\gamma_1}{2}\right)z^2 & \sqrt{3}\gamma_3(\{zx\} - i\{yz\}) & \frac{\sqrt{3}}{2}\gamma_2(x^2-y^2) - i\sqrt{3}\gamma_3\{xy\} & 0 \\ \sqrt{3}\gamma_3(\{zx\} + i\{yz\}) & -\frac{\gamma_1-\gamma_2}{2}(x^2+y^2) - \left(\gamma_2 + \frac{\gamma_1}{2}\right)z^2 & 0 & \frac{\sqrt{3}}{2}\gamma_2(x^2-y^2) - i\sqrt{3}\gamma_3\{xy\} \\ \frac{\sqrt{3}}{2}\gamma_2(x^2-y^2) + i\sqrt{3}\gamma_3\{xy\} & 0 & -\frac{\gamma_1-\gamma_2}{2}(x^2+y^2) - \left(\gamma_2 - \frac{\gamma_1}{2}\right)z^2 & -\sqrt{3}\gamma_3(\{zx\} - i\{yz\}) \\ 0 & \frac{\sqrt{3}}{2}\gamma_2(x^2-y^2) + i\sqrt{3}\gamma_3\{xy\} & -\sqrt{3}\gamma_3(\{zx\} + i\{yz\}) & -\frac{\gamma_1+\gamma_2}{2}(x^2+y^2) + \left(\gamma_2 - \frac{\gamma_1}{2}\right)z^2 \end{bmatrix}$$

$+$

$$\begin{bmatrix} \left(D_d - \frac{D_u}{3}\right)\mathrm{tr}\varepsilon + D_u\varepsilon_{zz} & \frac{2}{\sqrt{3}}D_u'(\varepsilon_{zx} - i\varepsilon_{yz}) & \frac{D_u}{\sqrt{3}}(\varepsilon_{xx} - \varepsilon_{yy}) - i\frac{2}{\sqrt{3}}D_u'\varepsilon_{xy} & 0 \\ \frac{2}{\sqrt{3}}D_u'(\varepsilon_{zx} + i\varepsilon_{yz}) & \left(D_d + \frac{D_u}{3}\right)\mathrm{tr}\varepsilon - D_u\varepsilon_{zz} & 0 & \frac{D_u}{\sqrt{3}}(\varepsilon_{xx} - \varepsilon_{yy}) - i\frac{2}{\sqrt{3}}D_u'\varepsilon_{xy} \\ \frac{D_u}{\sqrt{3}}(\varepsilon_{xx} - \varepsilon_{yy}) + i\frac{2}{\sqrt{3}}D_u'\varepsilon_{xy} & 0 & \left(D_d + \frac{D_u}{3}\right)\mathrm{tr}\varepsilon - D_u\varepsilon_{zz} & -\frac{2}{\sqrt{3}}D_u'(\varepsilon_{zx} - i\varepsilon_{yz}) \\ 0 & \frac{D_u}{\sqrt{3}}(\varepsilon_{xx} - \varepsilon_{yy}) + i\frac{2}{\sqrt{3}}D_u'\varepsilon_{xy} & -\frac{2}{\sqrt{3}}D_u'(\varepsilon_{zx} + i\varepsilon_{yz}) & \left(D_d - \frac{D_u}{3}\right)\mathrm{tr}\varepsilon + D_u\varepsilon_{zz} \end{bmatrix}$$

$$H^{86} =$$

$$\begin{bmatrix} -\frac{1}{\sqrt{2}}\left[P(x - iy) + iB(\{yz\} - i\{zx\}) + iC_2(\varepsilon_{yz} - i\varepsilon_{zx})\right] & 0 \\ \sqrt{\frac{2}{3}}\left[Pz - iB\{xy\} - iC_2\varepsilon_{xy}\right] & -\frac{1}{\sqrt{6}}\left[P(x - iy) + iB(\{yz\} - i\{zx\}) + iC_2(\varepsilon_{yz} - i\varepsilon_{zx})\right] \\ -\frac{1}{\sqrt{6}}\left[P(x + iy) - iB(\{yz\} + i\{zx\}) - iC_2(\varepsilon_{yz} + i\varepsilon_{zx})\right] & \sqrt{\frac{2}{3}}\left[Pz - iB\{xy\} - iC_2\varepsilon_{xy}\right] \\ 0 & \frac{1}{\sqrt{2}}\left[P(x + iy) - iB(\{yz\} + i\{zx\}) - iC_2(\varepsilon_{yz} + i\varepsilon_{zx})\right] \end{bmatrix}$$

$$H^{87} =$$

$$\begin{bmatrix}
-\sqrt{\frac{3}{2}}\gamma_3(\{zx\}-i\{yz\})-\sqrt{\frac{2}{3}}D_u'(\varepsilon_{xx}-i\varepsilon_{yx}) & -\sqrt{\frac{3}{2}}\gamma_2(x^2-y^2)+i\sqrt{6}\gamma_3\{xy\} \\
 & -\sqrt{\frac{2}{3}}D_u(\varepsilon_{xx}-\varepsilon_{yy})+\frac{4}{\sqrt{6}}iD_u'\varepsilon_{xy} \\
-\frac{1}{\sqrt{2}}\gamma_2(x^2+y^2)+\sqrt{2}\gamma_2z^2 & \frac{3}{\sqrt{2}}\gamma_3(\{zx\}-i\{yz\}) \\
-\frac{\sqrt{2}}{3}D_u(\varepsilon_{xx}+\varepsilon_{yy})+\frac{2\sqrt{2}}{3}D_u\varepsilon_{zz} & +\sqrt{2}D_u'(\varepsilon_{xx}-i\varepsilon_{yx}) \\
\frac{3}{\sqrt{2}}\gamma_3(\{zx\}+i\{yz\}) & \frac{1}{\sqrt{2}}\gamma_2(x^2+y^2)-\sqrt{2}\gamma_2z^2 \\
+\sqrt{2}D_u'(\varepsilon_{xx}+i\varepsilon_{yx}) & +\frac{\sqrt{2}}{3}D_u(\varepsilon_{xx}+\varepsilon_{yy})-\frac{2\sqrt{2}}{3}D_u\varepsilon_{zz} \\
\sqrt{\frac{3}{2}}\gamma_2(x^2-y^2)+i\sqrt{6}\gamma_3\{xy\} & -\sqrt{\frac{3}{2}}\gamma_3(\{zx\}+i\{yz\})-\sqrt{\frac{2}{3}}D_u'(\varepsilon_{xx}+i\varepsilon_{yx}) \\
+\sqrt{\frac{2}{3}}D_u(\varepsilon_{xx}-\varepsilon_{yy})+\frac{4}{\sqrt{6}}iD_u'\varepsilon_{xy} &
\end{bmatrix}$$

$$H^{66} = \begin{bmatrix} E_6 + Ap^2 + C_1 \operatorname{tr}\varepsilon & 0 \\ 0 & E_6 + Ap^2 + C_1 \operatorname{tr}\varepsilon \end{bmatrix}$$

$$H^{77} = \begin{bmatrix} E_7 - \frac{\gamma_1}{2}p^2 + D_d \operatorname{tr}\varepsilon & 0 \\ 0 & E_7 - \frac{\gamma_1}{2}p^2 + D_d \operatorname{tr}\varepsilon \end{bmatrix}$$

$$H^{76} =$$

$$-\frac{1}{\sqrt{3}}\begin{bmatrix} Pz + iB\{xy\} + iC_2\varepsilon_{xy} & P(x-iy)+iB(\{yz\}-i\{zx\})+iC_2(\varepsilon_{yz}-i\varepsilon_{zx}) \\ P(x+iy)+iB(\{yz\}+i\{zx\})+iC_2(\varepsilon_{yz}+i\varepsilon_{zx}) & -Pz-iB\{xy\}-iC_2\varepsilon_{xy} \end{bmatrix}$$

(12)

In Eq 12 the terms pertaining explicitly to the magnetic field have been omitted; x, y, z denote the Cartesian components of $\vec{p}$; the z-axis being parallel to crystal axis [001]. The brackets {ab} denote the symmetrised product (ab+ba)/2. Zincblende structure has no inversion centre and therefore k-linear terms are allowed in the energy dispersion. As they are small however, they have also been omitted in Eq 12.

the terms pertaining explicitly to the magnetic field have been omitted; x, y, z denote the Cartesian components of $\tilde{p}$; the z-axis being parallel to crystal axis [001]. The Luttinger parameters are understood to be replaced by $\gamma_i \Rightarrow \hbar^2/m\ \gamma_i$. The brackets {ab} denote the symmetrised product (ab+ba)/2. Zincblende structure has no inversion centre and therefore k-linear terms are allowed in the energy dispersion. As they are small however, they have also been omitted

Most lead chalcogenides crystallise in rock salt structure and have a small direct gap at the L-point of the Brillouin zone. As they have an inversion centre all levels are doubly degenerate.

$G_{[111]} = D_3$

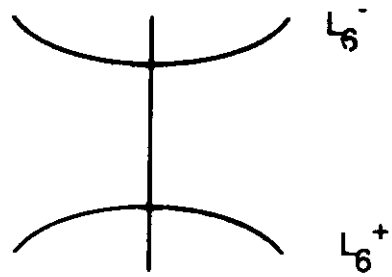

1, 2, 3 denote the components of a Cartesian co-ordinate system with 3 parallel to the main valley axis (a (111)axis).

$$H =$$

$$\begin{bmatrix} E^- + \frac{p_1^2 + p_2^2}{2m_t^-} + \frac{p_3^2}{2m_l^-} & 0 & P_l p_3 & P_t(p_1 - \mathrm{i}p_2) \\ 0 & E^- + \frac{p_1^2 + p_2^2}{2m_t^-} + \frac{p_3^2}{2m_l^-} & P_t(p_1 + \mathrm{i}p_2) & -P_l p_3 \\ P_l p_3 & P_t(p_1 - \mathrm{i}p_2) & E^+ - \frac{p_1^2 + p_2^2}{2m_t^+} - \frac{p_3^2}{2m_l^+} & P_t(p_1 - \mathrm{i}p_2) \\ P_t(p_1 + \mathrm{i}p_2) & -P_l p_3 & P_t(p_1 + \mathrm{i}p_2) & E^+ - \frac{p_1^2 + p_2^2}{2m_t^+} - \frac{p_3^2}{2m_l^+} \end{bmatrix}$$

$$+$$

$$\begin{bmatrix} D_d^- \operatorname{tr}\varepsilon + D_u^- \varepsilon_{33} + g_l^- \mu_B B_3 & g_t^- \mu_B (B_1 - \mathrm{i}B_2) & 0 & 0 \\ g_t^- \mu_B (B_1 + \mathrm{i}B_2) & D_d^- \operatorname{tr}\varepsilon + D_u^- \varepsilon_{33} - g_l^- \mu_B B_3 & 0 & 0 \\ 0 & 0 & D_d^{g-t} \operatorname{tr}\varepsilon + D_u^{+-} \varepsilon_{33} + g^{g-t} \mu_B B_3 & g_t^{+g} \mu_B (B_1 - \mathrm{i}B_2) \\ 0 & 0 & g_t^+ \mu_B (B_1 + \mathrm{i}B_2) & D_d^{+g} \operatorname{tr}\varepsilon + D_u^{+g} \varepsilon_{33} - g_l^{+g} \mu_B B_3 \end{bmatrix} \tag{13}$$

1, 2, 3 denote the components of a Cartesian co-ordinate system with 3 parallel to the main valley axis (a (111)axis).

Let V be the crystal potential for material A and V+ δV the potential for material B. Due to the similarity of A and B δV will be small. Then in first order perturbation theory

$$\left(\frac{p^2}{2m} + V + V_{spinorbit}\right) u_{nk_0} = E_{nk_0}$$

$$E_{nk_0}{}^{A} = E_{nk_0}$$

$$E_{nk_0}{}^{B} = E_{nk_0} + \int_{\Omega} u_{nk_0}{}^{*} \delta V u_{nk_0} d^3r$$

$$u_{nk_0}{}^{B} = u_{nk_0}{}^{A} = u_{nk_0}$$

Ω denotes a unit cell. The continuity of the wave function $\Psi(\vec{r})$ requires due to the orthogonality of u_n the continuity of each envelope function f_n because by multiplying with u and integrating over a unit cell to the left and the right of the interface one obtains

$$\int_{\Omega l} u_n{}^{*} \Psi d^3r = \int_{\Omega r} u_n{}^{*} \Psi d^3r$$

$$\int_{\Omega l} u_n{}^{*} \sum_{n'} u_{n'} f_{n'}{}^{l} d^3r = \int_{\Omega r} u_n{}^{*} \sum_{n'} u_{n'} f_{n'}{}^{r} d^3r$$

$$f_{n'}{}^{l} = f_{n'}{}^{r} \quad , n' = 1, \ldots$$

matching conditions

$$f_{n>N} = -\frac{1}{E_n - E}\sum_{n'\le N}\vec{P}_{nn'}\cdot\vec{p}f_{n'} \quad \text{continuous}$$

Multiplying by the constants $\vec{P}_{n'n}$ and summing over all n>N

$$\sum_{n'<N}\sum_{\alpha}Q^{\alpha z}_{nn'}\frac{\partial}{\partial z}f_{n'} \qquad \text{continuous}$$

z direction perpendicular to the interface
and α = x,y,z

one band approximation (N=1)

$$\frac{1}{m_l^*}\frac{\partial}{\partial z}f = \frac{1}{m_r^*}\frac{\partial}{\partial z}f$$

$$\frac{1}{m_z^*} = \sum_{n>1}\sum_{\alpha}\frac{P_\alpha^* P_z}{E_n - E_1}$$

continouity condition may be to stringent:
Γ-point

interface should be perpendicular to the x axis (crystallographic [100]) and the inplane momentum in direction z is equal to zero. The 8×8 Hamiltonian matrix reduces to two 4×4 problems of the form

$$\begin{bmatrix} E_6 - E & -Pk_+/\sqrt{2} & -Pk_+/\sqrt{6} & -Pk_-/\sqrt{3} \\ -Pk_-/\sqrt{2} & E_8 - E & 0 & 0 \\ -Pk_-/\sqrt{6} & 0 & E_8 - E & 0 \\ -Pk_+/\sqrt{3} & 0 & 0 & E_7 - E \end{bmatrix} \begin{bmatrix} f_1 \\ f_3 \\ f_5 \\ f_8 \end{bmatrix} = 0$$

$$k_\pm = k_x \pm i k_y$$

not all four functions can be continuous if Eg and E7 change by a different amount across the interface

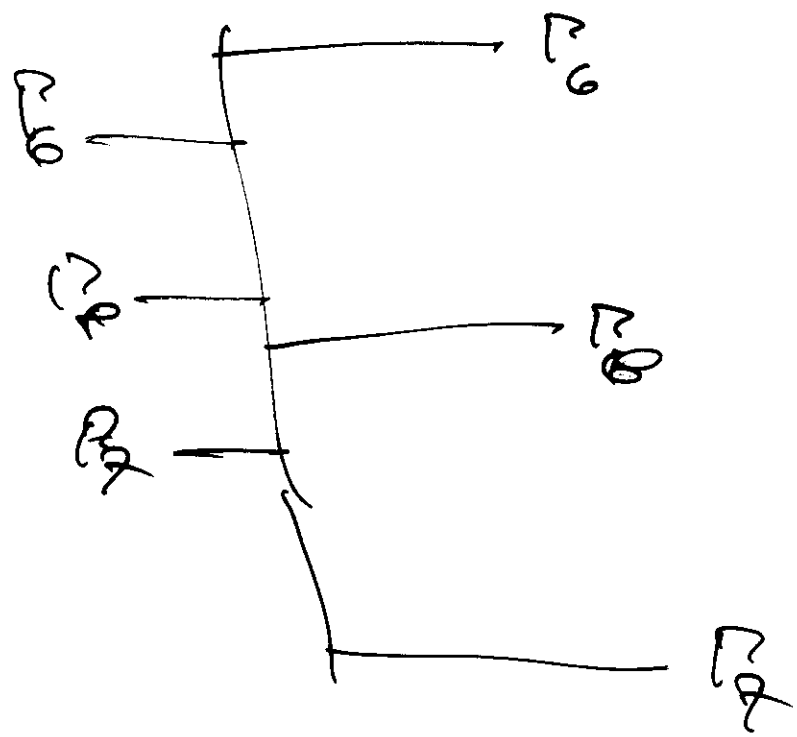

The matching conditions for the derivatives ~~must~~ should not have a significant influence on the results of a boundary value problem. To see this we observe first that although the N×N Hamiltonian with quadratic terms has 4N linearly independent solutions to a given energy E only 2N are reasonable in EFA theory. To see this consider a bulk material The solutions of the differential equations are exponential functions and the operators are replaced by numbers. and they are reduced to an algebraic problem of N^{th} order in E and $(4N)^{th}$ order in p allowing 4N solutions for p for a given energy E. However for each band only two values of k ($=k_0 \pm \delta k$) close to k_0 are reasonably described by EFA whereas for the other two lying far away EFA does not describe the bulk energy dispersion at all. Thus if it turns out in an actual calculation that the amplitudes of these additional states are large the results of the whole calculation are meaningless and EFA cannot describe this physical situation.

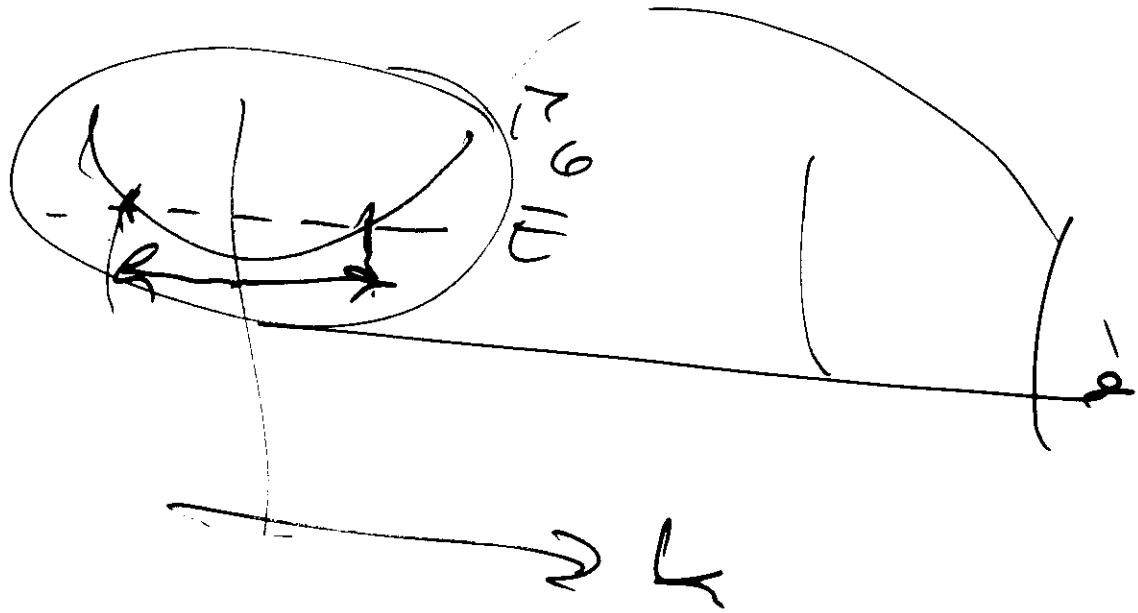

The change from layer A to layer B at an interface is not abrupt but occurs gradually

The envelope functions are continuous differentiable functions

$$\vec{P}\cdot\vec{p} \Rightarrow \tfrac{1}{2}\left(\vec{P}\cdot\vec{p}+\vec{p}\cdot\vec{P}\right),$$
$$Qp_\alpha p_\beta \Rightarrow p_\alpha Q p_\beta$$

Bloch condition:

$$f_n(x,y,z+D) = \exp(\mathrm{i}\,KD) f_n(x,y,z),\ \ n=1,\ldots N$$
$$K \in [-\pi/D, \pi/D]$$

vanishing in-plane momentum:

$$\cos(KD) = -\frac{1}{2}\left[\frac{T}{S}+\frac{S}{T}\right]\sin(k_{zA}d_A)\sin(k_{zB}d_B) + \cos(k_{zA}d_A)\cos(k_{zB}d_B)$$

$$S = \frac{k_{3A}}{E_A^+ + k_t^{\,2}/2m_t^+ + k_3^{\,2}/2m_t^+ - E}$$

for the L-point

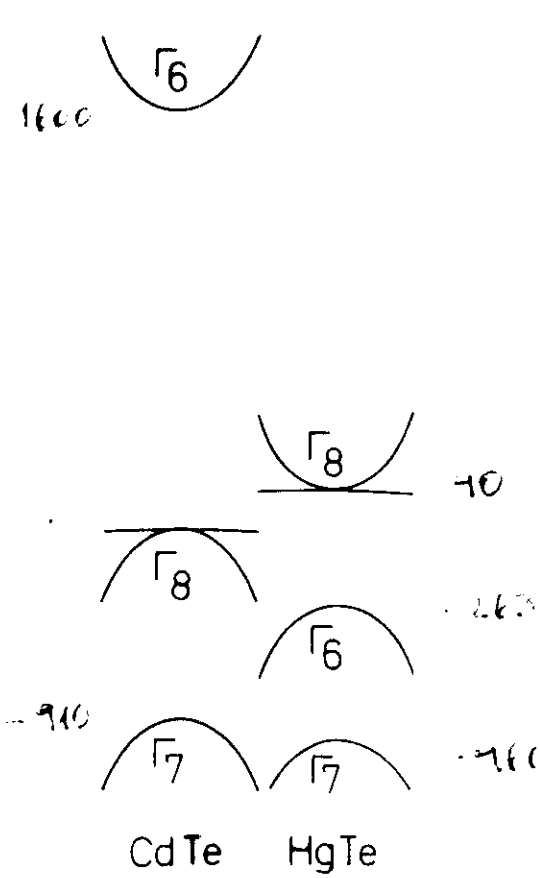
Γ6
Γ8
Γ8
Γ6
Γ7
Γ7
CdTe
HgTe

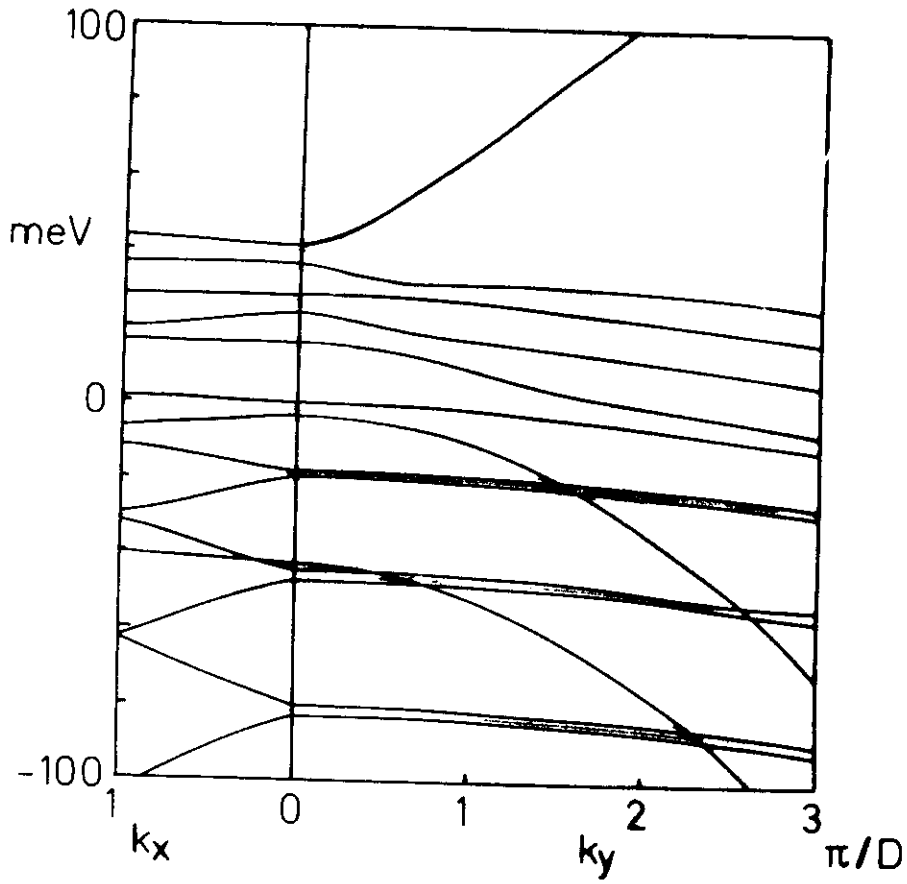
100
meV
0
-100
1
0
1
2
3
kx
ky
π/D

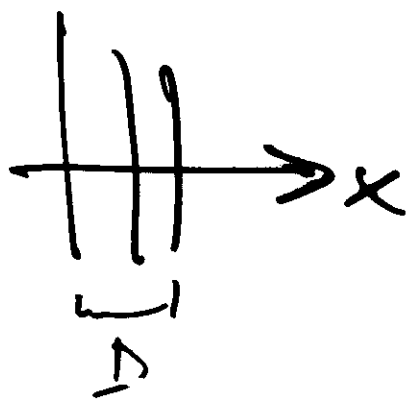
x
Δ

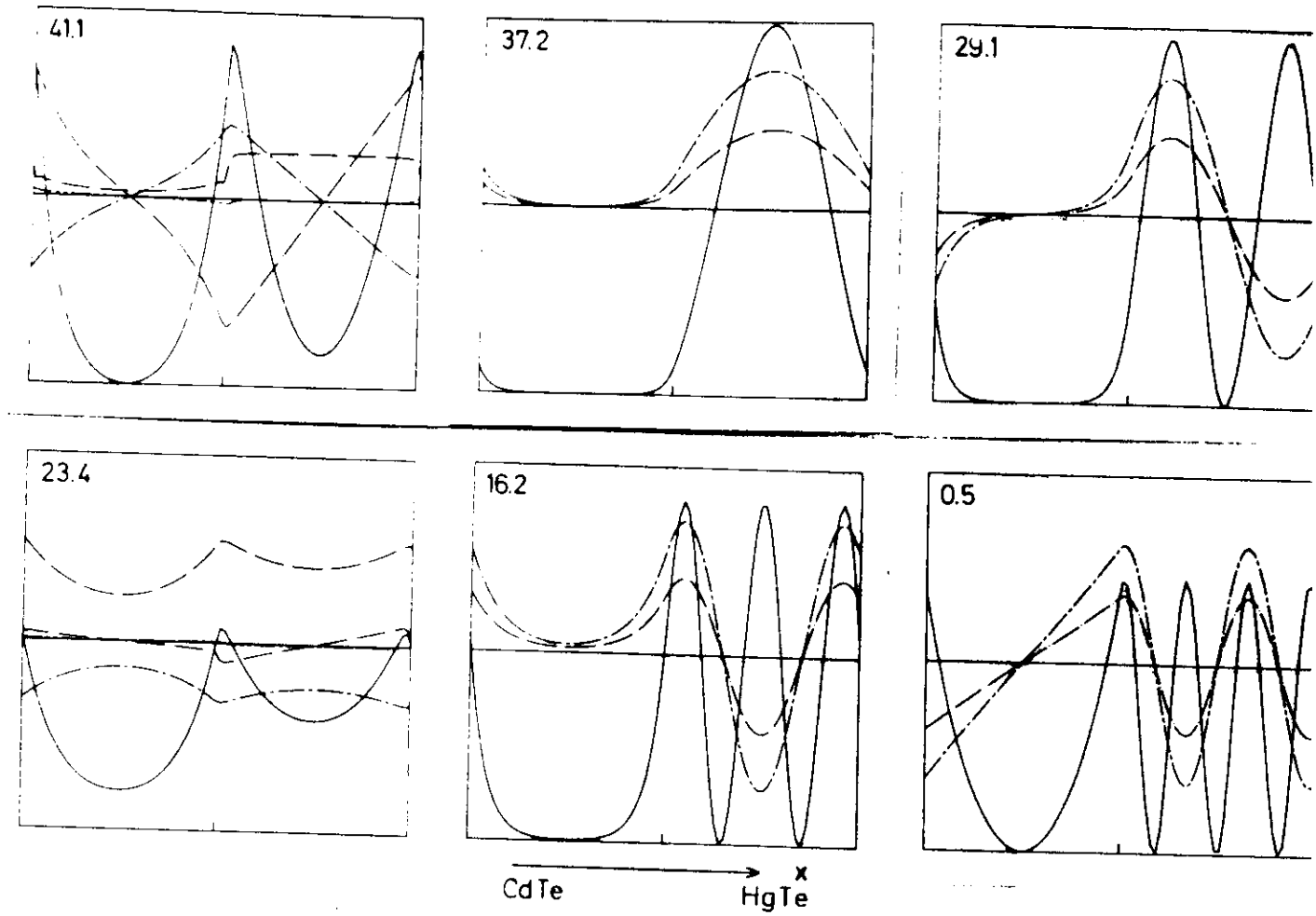

15/15 mm

SPLINE FUNCTIONS

Interpolate between n data points (x_i,y_i) (i=1,...n)
by means of a function g(x)
with k≤n continuous derivatives
and make

$$\sigma \equiv \int_a^b \left[g^{(k)}(x)\right]^2 dx \text{ as small as possible}$$

$$a \le x_1 < x_2 < \ldots < x_n \le b$$

For k>n no unique solution
for k=n Lagrangian interpolation polynomial (k-1)
for k<n unique solution:
g(x) is a piece wise function given in any interval
$[x_i,x_{i+1}]$ by a polynomial of degree at most 2k-1,
the $0^{th}..(2k-2)^{th}$ derivative of the polynomial arcs
join smoothly at every x_i
in intervals $(-\infty,x_1)$ and (x_n,∞) degree k-1
g(x) is a *natural Spline s* of degree 2k-1

Let

$$\mathcal{L}[f] \equiv \sum_{r=0}^{k-1} \int_a^b f^{(r)}(x)\,d\mu_r(x), \quad \mu_r(x) \text{ bounded variation}$$

for arbitrary $\mathcal{L}$ $\mathcal{L}(s)$ is the best approximation to $\mathcal{L}(f)$

$$\forall s\colon\ s(x) = P_{k-1}(x) + \sum_{j=1}^{n} c_j \left(x - x_j\right)_+^{2k-1} \text{ uniquely given}$$

B-splines:

$$g_l(s;t) \equiv (s-t)_+^{l-1}$$

$$g_l(t_0,t_1,\ldots t_n;t) \equiv \frac{g_l(t_1,\ldots t_n;t) - g_l(t_0,\ldots t_{n-1};t)}{t_n - t_0}$$

$$M_{0,l}(t) \equiv g_l(t_0,t_1,\ldots t_l;t) \qquad B-spline$$

$$B_{0,l}(t) \equiv M_{0,l}(t)(t_l - t_0) \qquad normalized\ B-spline$$

$$s_{k-1}(x) = P_{k/2-1}(x) + \sum_{i=1}^{n} A_i M_{i,k}(x) \qquad uniquely$$

for multiplicity n of x_j is the $(k-n)^{th}$ derivative of $M_{.,k}(x_j)$ discontinuous

$$ge(t_0 t_1 t_j t) = \frac{ge(t_1,t) - ge(t_j,t}{t_1 - t_0}$$

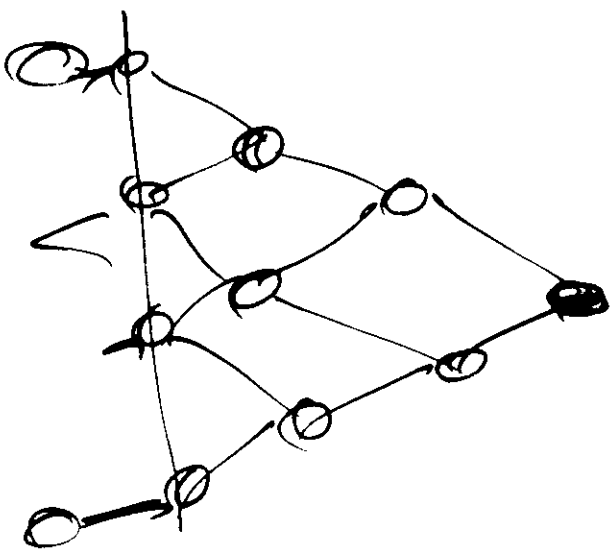

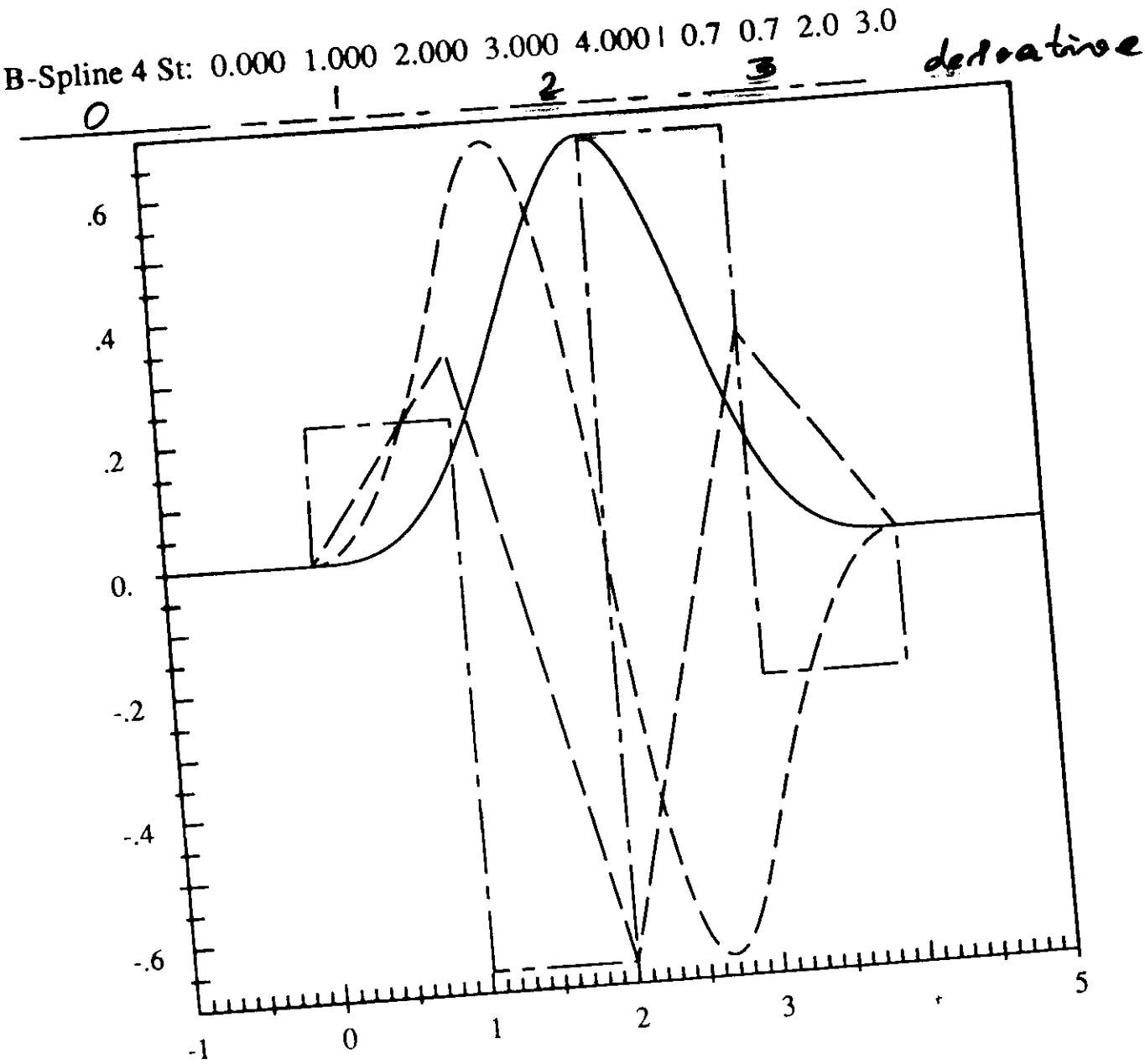
B-Spline 4 St: 0.000 1.000 2.000 3.000 4.000 0.7 0.7 2.0 3.0
0
1
2
3
derivative
.6
.4
.2
0.
-.2
-.4
-.6
-1
0
1
2
3
5

B-Spline 4 St: 0.000 1.000 3.000 3.000 4.000 | 0.6 1.0 2.0 2.0

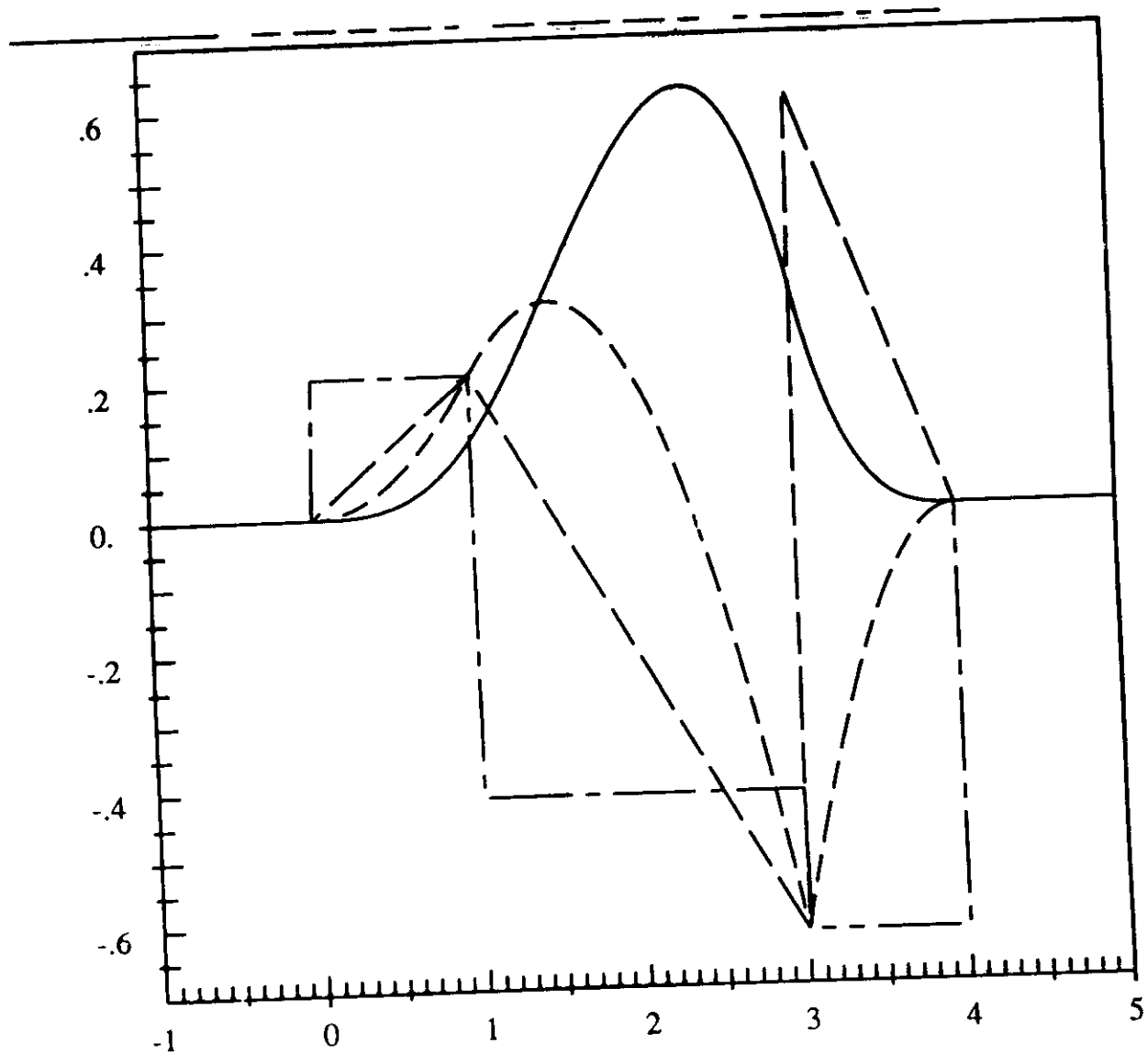

B-Spline 4 St: 0.000 3.000 3.000 3.000 4.000 | 1.0 2.9 5.9 6.0

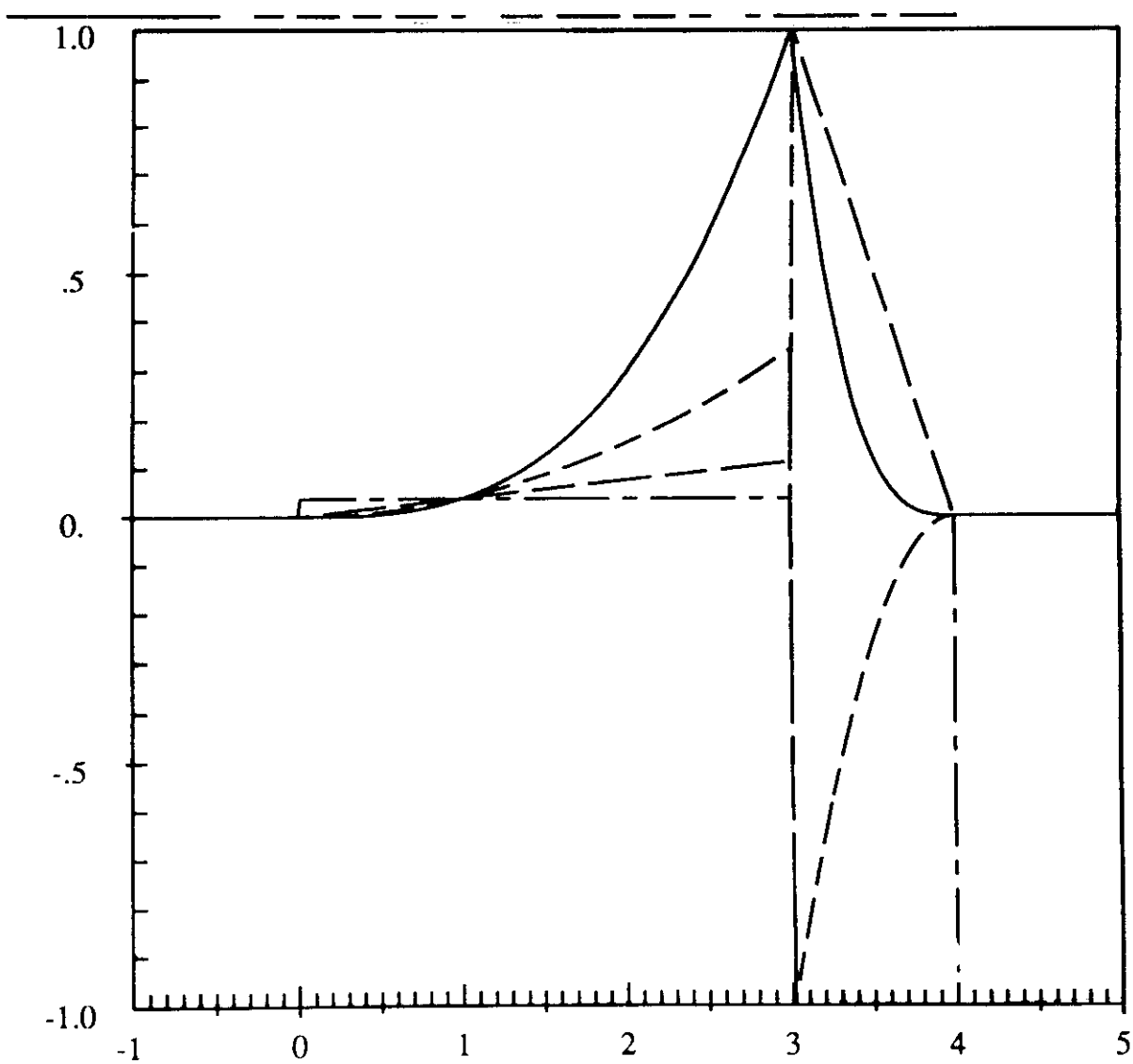

B-Spline 4 St: 0.000 4.000 4.000 4.000 4.000 | 1.0 0.8 0.4 0.1

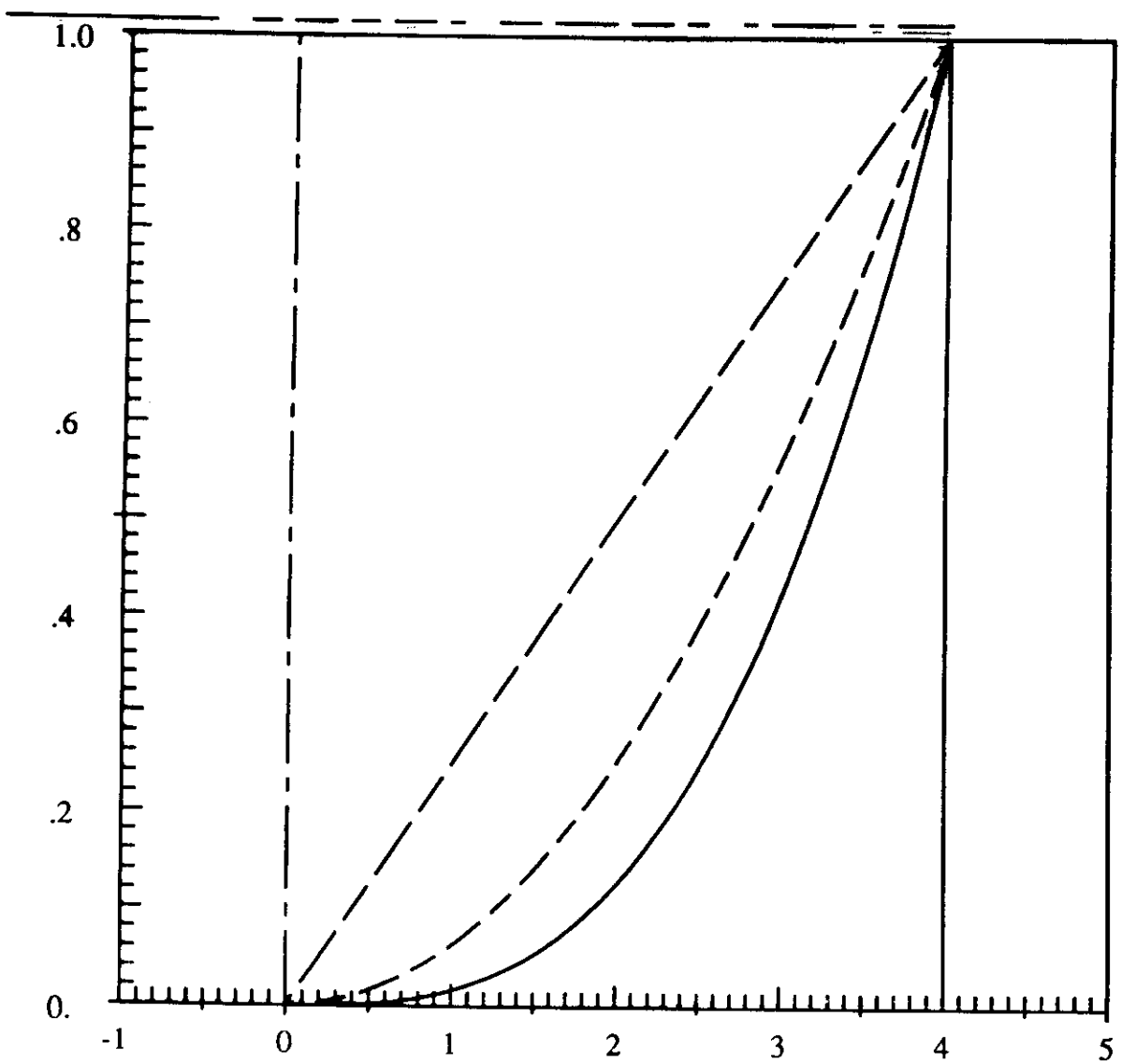

B-Spline 4 St: 0.000 2.999 3.000 3.001 4.0001 1.0 2.9 3997. 4.E+06

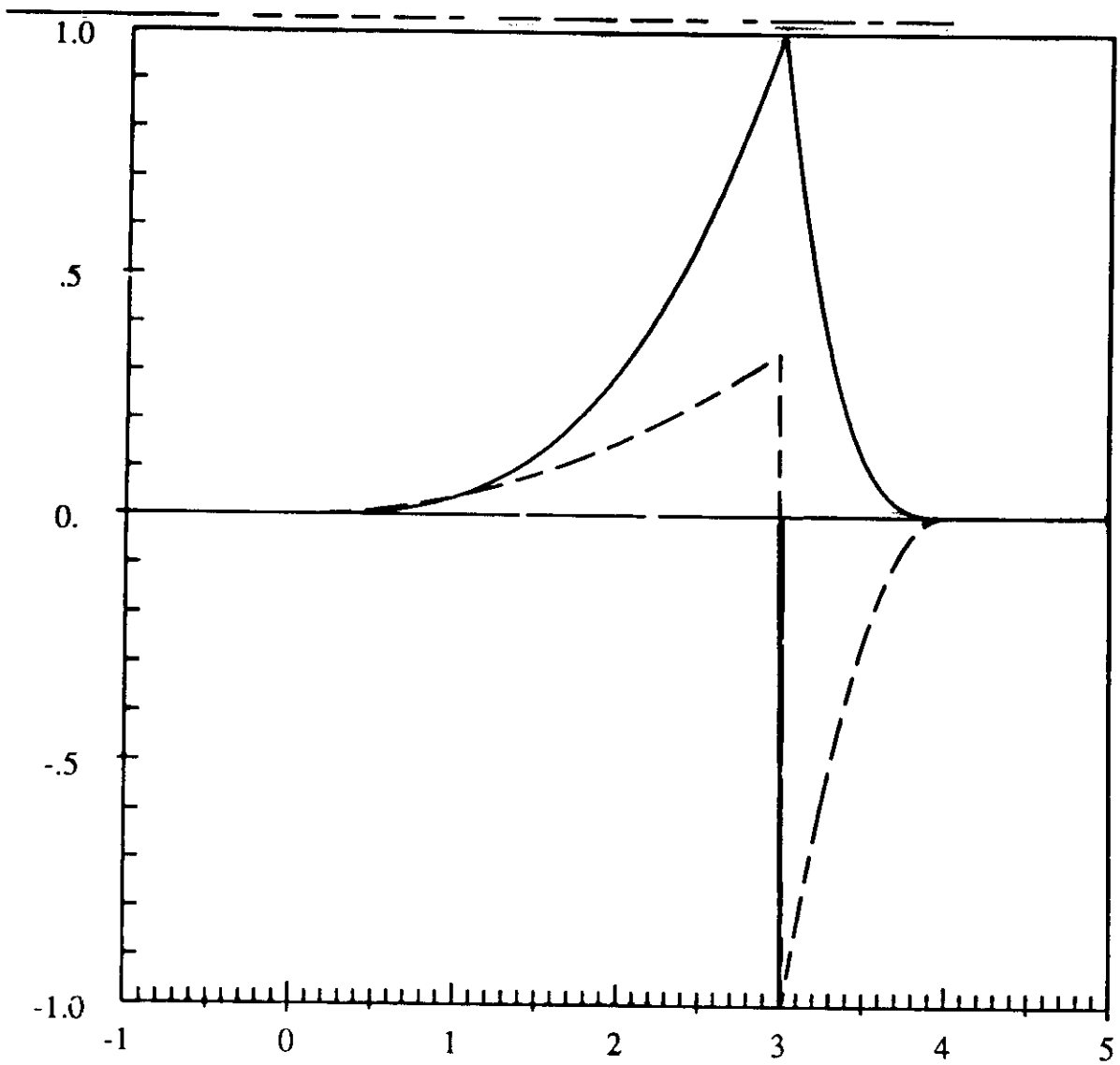

Why PbTe-EuTe Heterostructures ?

- ➞ PbTe/$Pb_{1-x}Eu_xTe$ has been used for mid-IR quantum well diode lasers, type I heterostructure system with very high mobilities in the PbTe QW,

- ➞ PbTe and EuTe is a combination of
  a ***narrow gap*** (PbTe: E_g = 0.2 eV) and
  a ***wide gap*** (EuTe: E_g = 2.0 eV material
  resulting in very large confinment energies,

- ➞ PbTe and EuTe is a combination of
  a ***diamagnetic*** (PbTe) and
  a ***antiferromagnetic*** (EuTe) material,
  investigation of *"magnetic"* superlattices,

- ➞ Investigation of the structural properties of short period EuTe/PbTe SL,

- ➞ EuTe layers can be used as ***insulation*** layers in IV-VI heterostructures,

PbTe/EuTe Superlattice

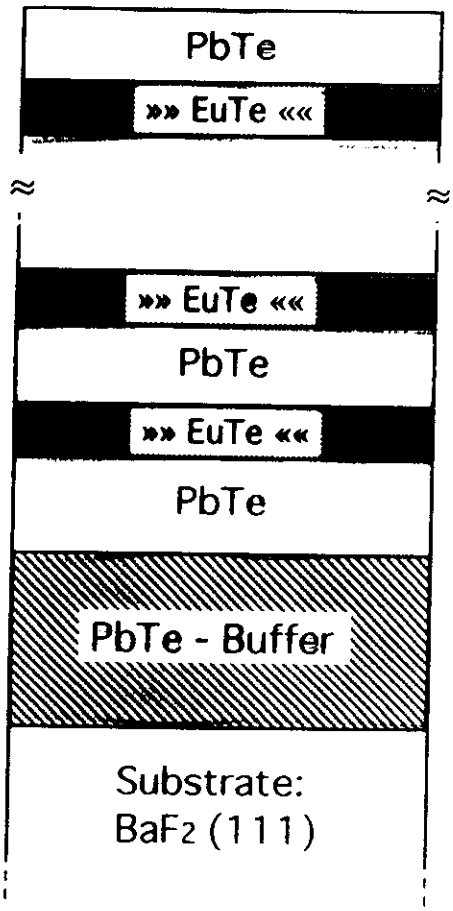

MBEG182:

40 Periods

Period:	345.48Å
PbTe:	325.77Å
	= 87.3ml
EuTe:	19.71Å
	= 5.0 ml
a_{PbTe}:	6.462Å
a_{EuTe}:	6.598Å
$\Delta a/a$:	2.1%

EuTe strained with
a_{normal}=6.828Å

Buffer: PbTe, 4μm relaxed

Type I MQW **Photodetector: Interband Transitions**

$PbTe/Pb_{1-x}Eu_xTe$ (x<7%)

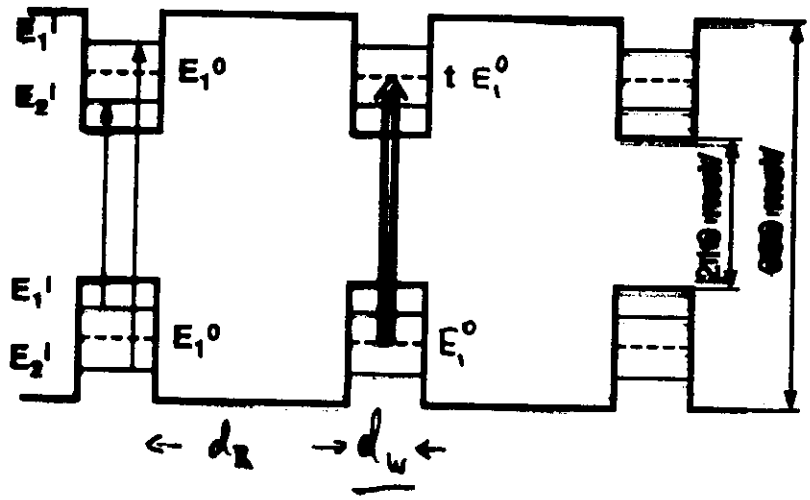

for growth along [111]: 2 sets of subbands
"l" longitudinal valleys
"θ" oblique valleys

Type II MQW (staggered)

$PbSe/Pb_{1-x}Mn_xSe$

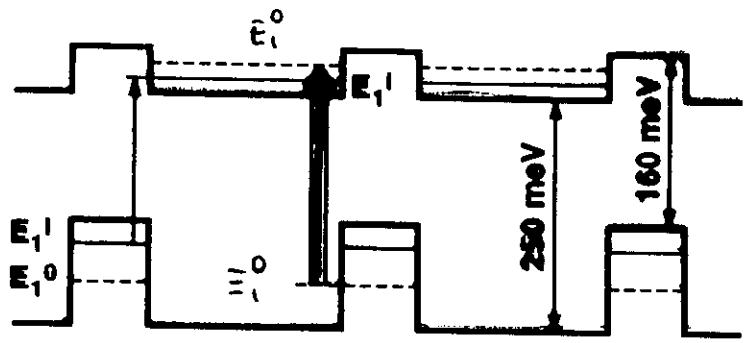

MQW DETECTORS FOR THE INFRARED:

- conventional technology for thermal imaging relies mainly on **Hg1-xCdxTe**

  disadvantage: extremely precise control of composition for $\lambda > 10\ \mu m$ necessary.

- IV-VI compounds like PbSe, PbS still in use both as polycristalline bulk materials as well as singlecrystalline epitaxial films: in particular PbSe, PbSnSe on Silicon substrates as photovoltaic detectors for IR focal plane arrays Zogg et al. (cut off frequency: > 100 MHz).

- MQW detectors relying on <u>intersubband</u> transitions: photoconductive, broad response
  <u>interbandtransitions:</u> step-like changes of the photoconductivity whenever $\hbar\omega$ corresponds to transition energy (type I band alignment).

GROWTH DIRECTION

Z ∥ [001]
(Substrates: PbTe, GaAs, NaCl)

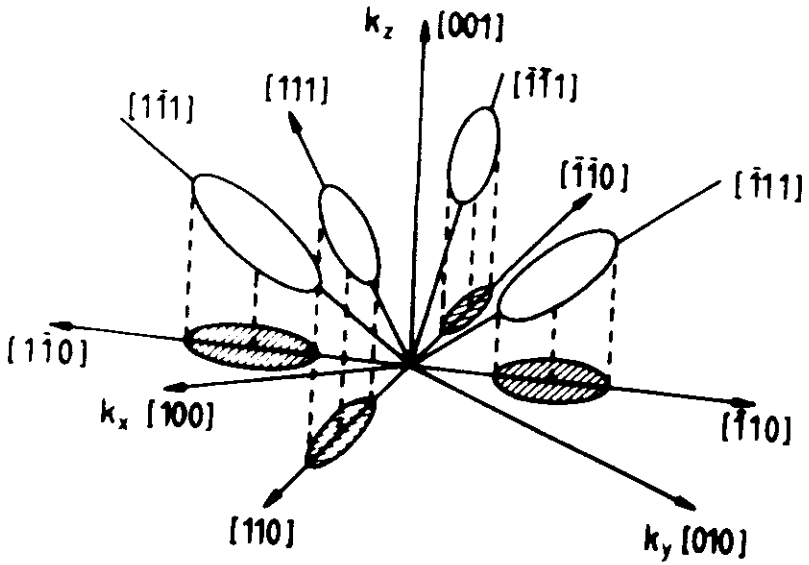

Z ∥ [111]
(Substrates: BaF_2)

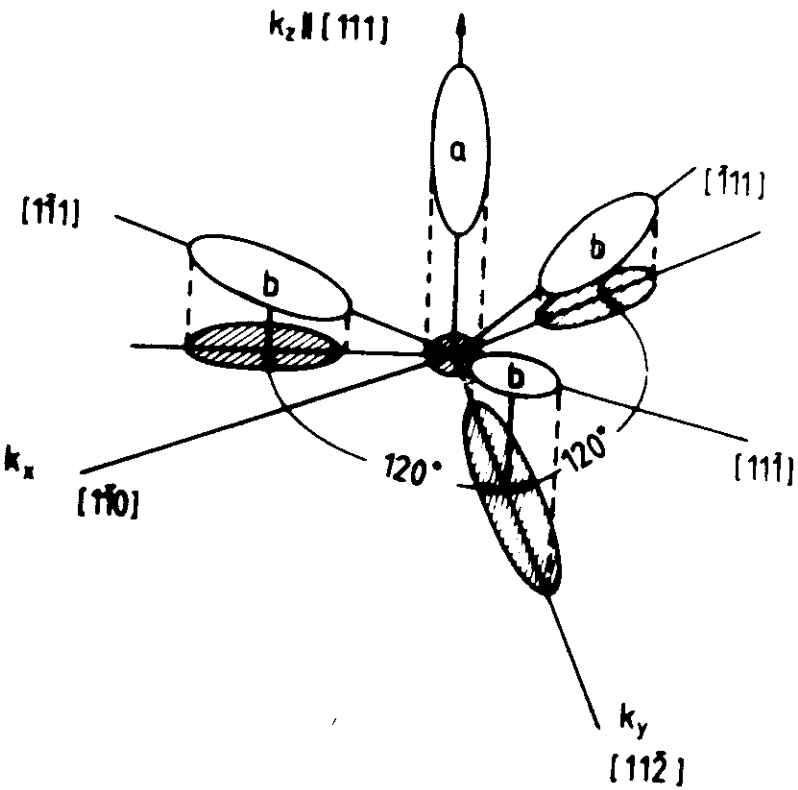

PET148 2 STKL, Spline Wed Jul 21 15:43:57 1993 fileout: PET14866a
WR 1 1 1 Tal 1 1 1
E_g d Konz Stst E_ps Ps/Pp mtc mlc mtv mlv
189.7 9.3 0.000 7 6.02 3.42 0.06 0.50 0.10 0.92
361.0 64.8 0.029 28 5.55 3.70 0.06 0.50 0.10 0.92
Exchange: B, b1, A, a1 2.2 1.2 9.0 8.0
LtgsbdOffset: 0.500 kx=0, ky=0, E vs kz [pi/D]

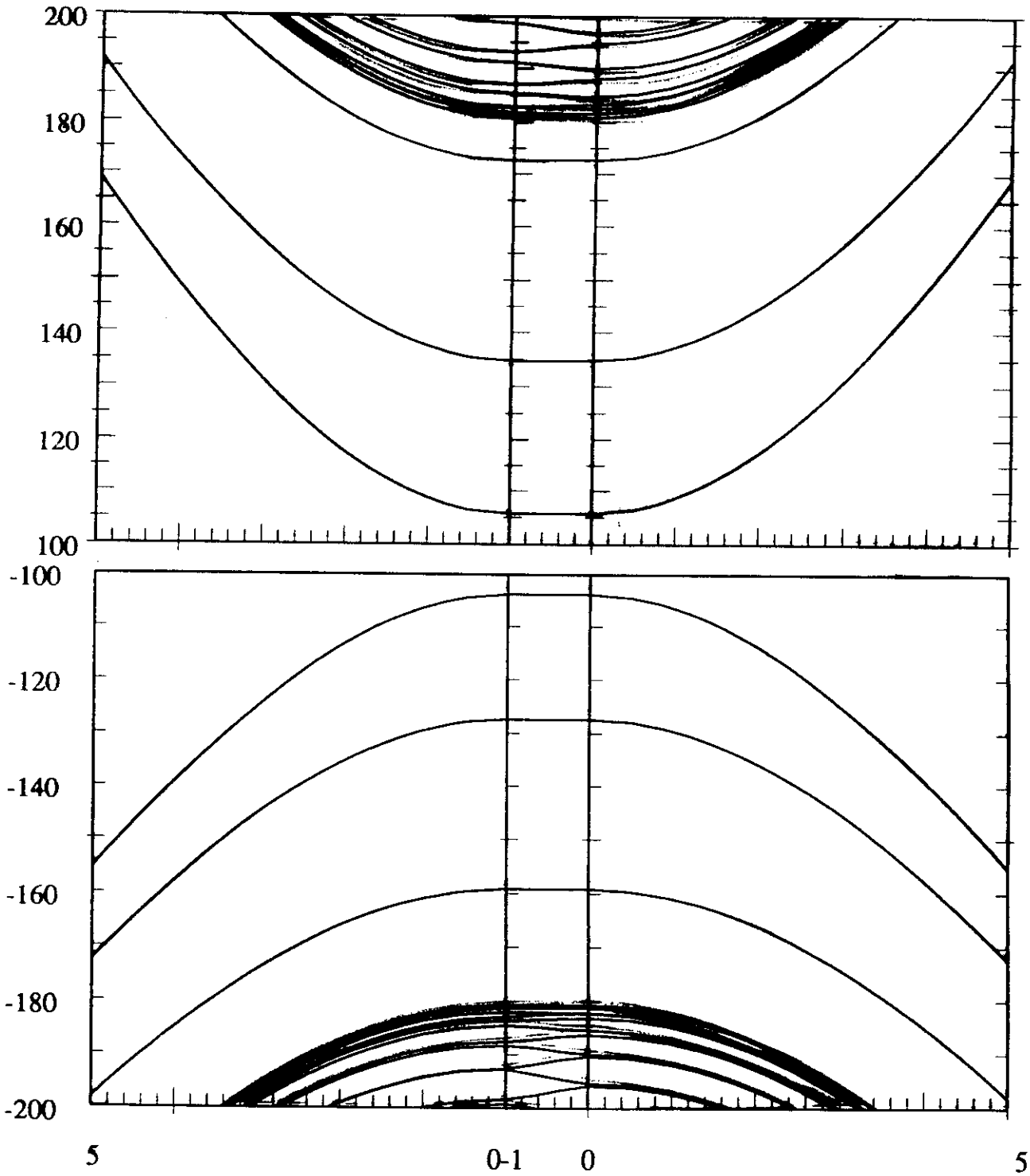

Energie [meV] vs k [pi/D] inplane SG inplane

PET148 2 STKL, Spline Wed Jul 21 15:45:19 1993 fileout: PET14864a
WR 1 1 1 Tal 1 1 -1
E_g d Konz Stst E_ps Ps/Pp mtc mlc mtv mlv
189.7 9.3 0.000 4 6.02 3.42 0.06 0.50 0.10 0.92
361.0 64.8 0.029 13 5.55 3.70 0.06 0.50 0.10 0.92
Exchange: B, b1, A, a1 2.2 1.2 9.0 8.0
LtgsbdOffset: 0.500 kx=0, ky=0, E vs kz [pi/D]

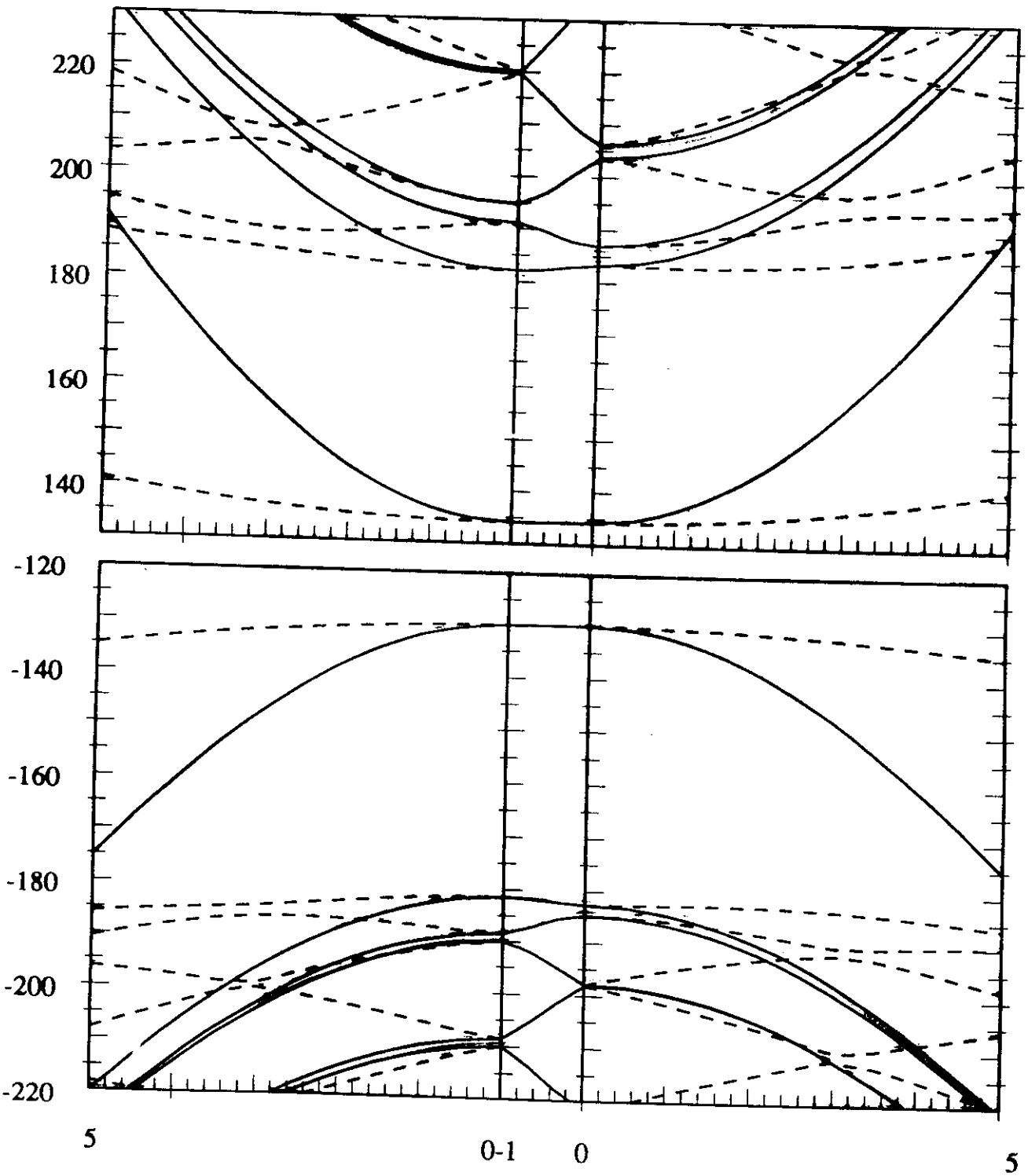

Energie [meV] vs k [pi/D] inplane SG inplane

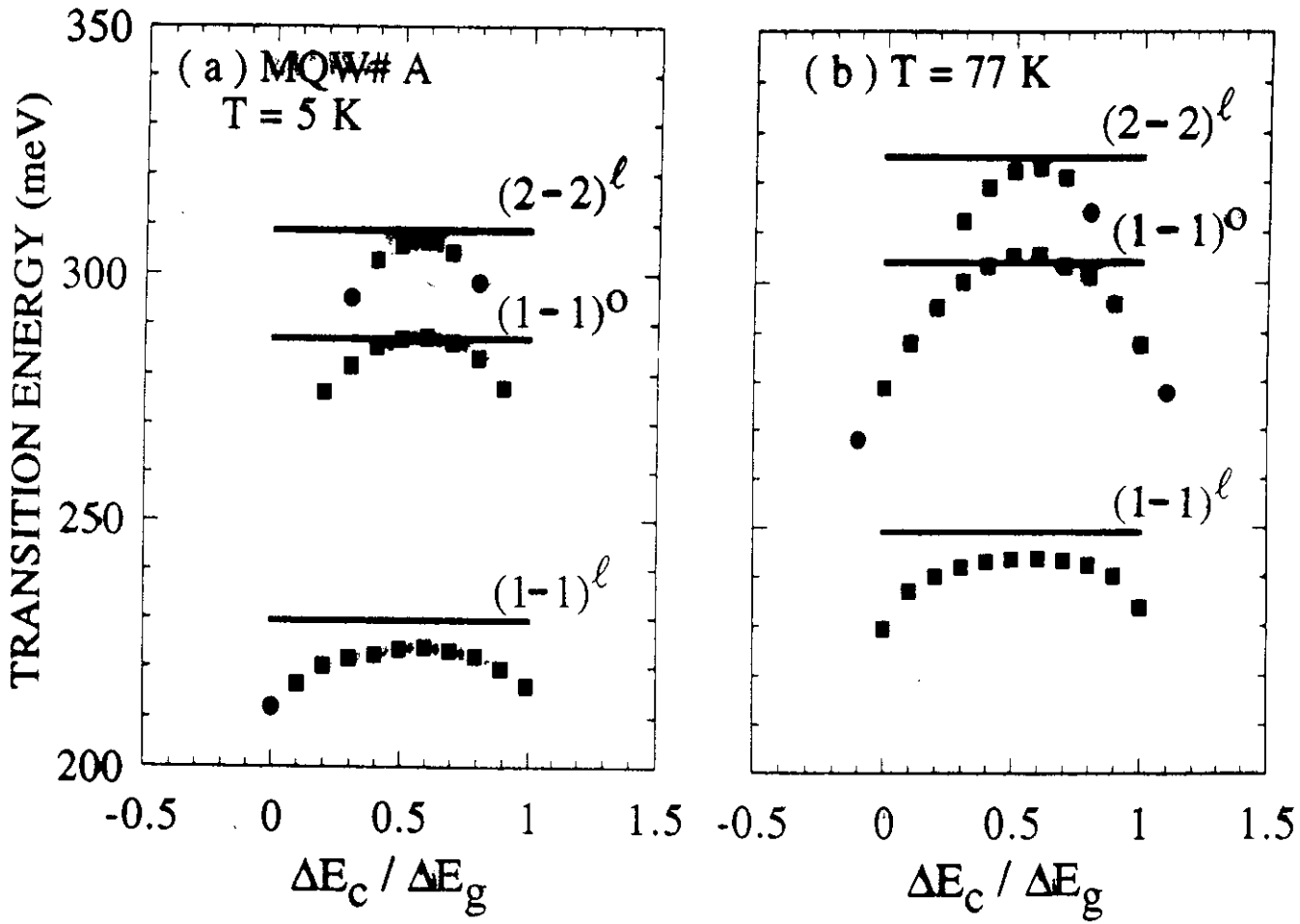
(a) MQW# A
T = 5 K
(b) T = 77 K
(2-2)ℓ
(1-1)o
(1-1)ℓ
TRANSITION ENERGY (meV)
350
300
250
200
-0.5
0
0.5
1
1.5
ΔEc / ΔEg

206

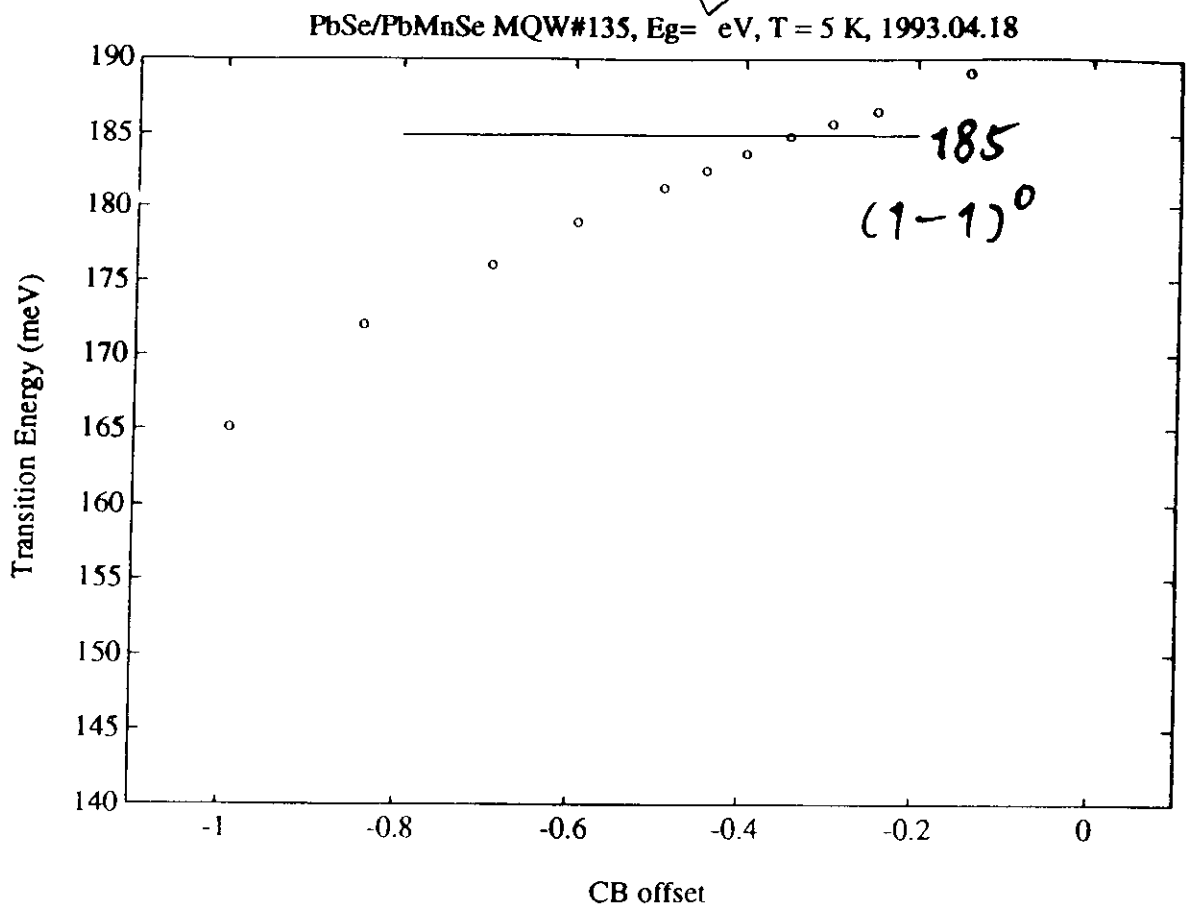
PbSe/PbMnSe MQW#135, Eg= eV, T = 5 K, 1993.04.18
Transition Energy (meV)
CB offset
185
(1-1)0

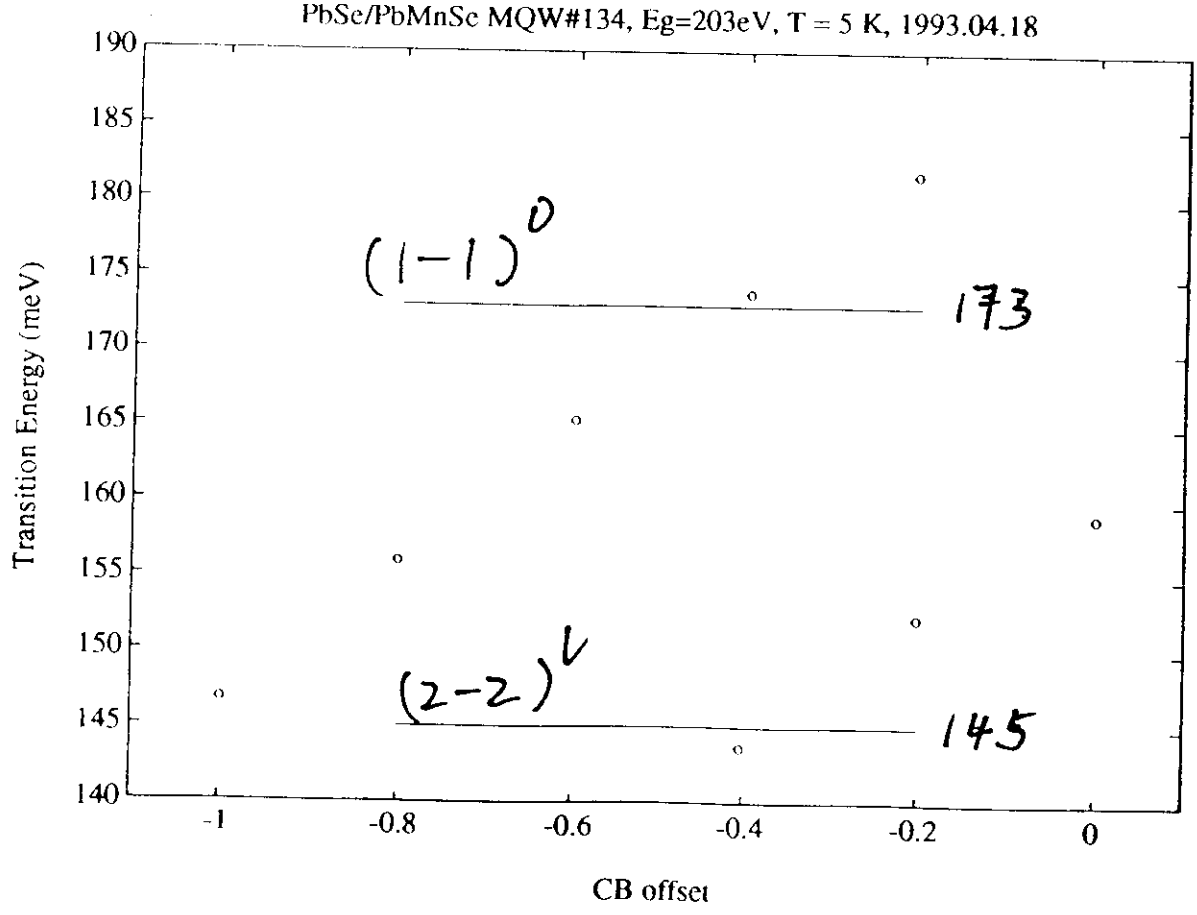
PbSe/PbMnSe MQW#134, Eg=203eV, T = 5 K, 1993.04.18
Transition Energy (meV)
CB offset
(1-1)0
173
(2-2)V
145

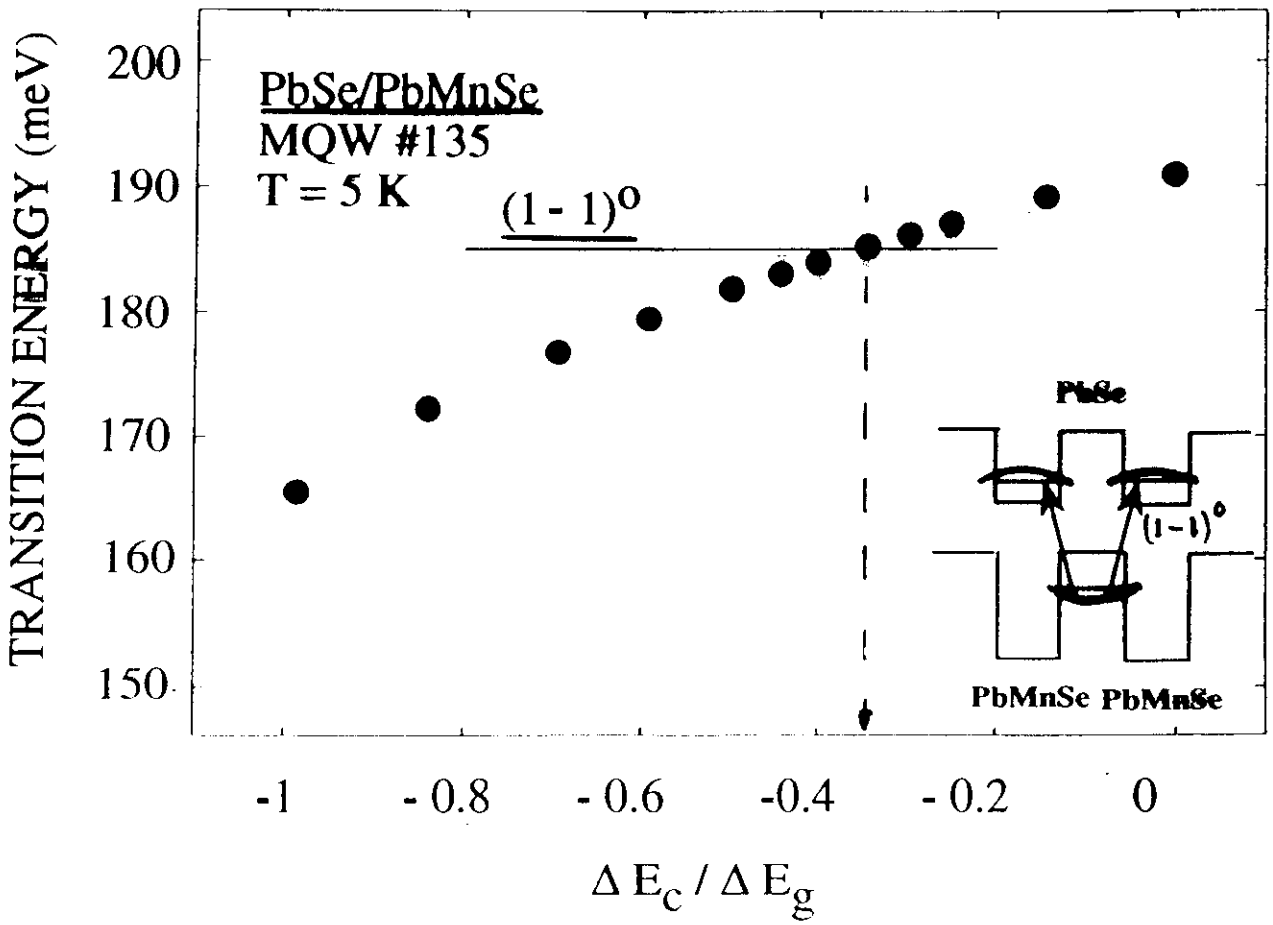
PbSe/PbMnSe
MQW #135
T = 5 K
(1 - 1)°
TRANSITION ENERGY (meV)
200
190
180
170
160
150
-1
- 0.8
- 0.6
-0.4
- 0.2
0
ΔE_c / ΔE_g
PbSe
(1-1)°
PbMnSe PbMnSe

Absorption constant

$$\varepsilon = \varepsilon^{BG} + \delta\varepsilon^{VB-CB}$$

$$\alpha = -\frac{1}{\mathcal{E}}\frac{d\mathcal{E}}{dz} = -\frac{1}{\mathcal{E}}\frac{n}{c}\frac{dN\hbar\omega}{dt}$$

$$\mathcal{E} = \frac{n^2\omega^2}{2\pi c^2}A_0^2$$

$$S = I(\omega)\Delta\omega = \frac{\omega^2}{2\pi n}A_0^2$$

$$\frac{1}{t}|a_{fi}|^2 = \frac{4\pi^2 e^2}{\omega^2 c}\frac{I(\omega)}{n}\frac{1}{\hbar^2}\left|\left\langle f\left|\frac{\mathbf{p}_E}{m}\right|i\right\rangle\right|^2$$

$$dI\Delta\omega = d\mathcal{E}\frac{c}{n} = -\frac{1}{2\pi^3}\int d^3k\frac{1}{t}|a_{fi}|^2\delta\left(\frac{E_f - E_i - \hbar\omega}{\hbar}\right)\Delta\omega\hbar\omega dz\frac{n}{c}\frac{c}{n}$$

$$\alpha(\omega) = \frac{4\pi^2 e^2}{c\omega n}\frac{1}{(2\pi)^3}\int d^3k\delta\left(E_f - E_i - \hbar\omega\right)\left|\left\langle f\left|\dot{\mathbf{r}}_E\right|i\right\rangle\right|^2\left(f_i - f_f\right)$$

$$\dot{\mathbf{r}} = \frac{1}{i\hbar}[\mathbf{r}, H] = \frac{1}{\hbar}\frac{\partial H}{\partial \mathbf{k}}$$

$$\varepsilon = \varepsilon_1 + i\varepsilon_2,$$

$$\varepsilon_1 = n^2 - \frac{c^2}{\omega^2}\frac{\alpha^2}{4},$$

$$\varepsilon_2 = \frac{cn}{\omega}\alpha$$

$$n(\omega) - n_\infty = (c/\pi)P\int_0^\infty \alpha(\omega')\left(\omega'^2 - \omega^2\right)^{-1}d\omega'$$

MQW148 5 STKL, Spline Fri Jul 16 13:28:04 1993 fileout: MQW14866a

WR 1 1 1 Tal 1 1 1 epsinf 1.0

E_g	d	Konz	Stst	E_ps	Ps/Pp	mtc	mlc	mtv	mlv
189.7	9.3	0.000	13	6.02	3.42	0.06	0.50	0.10	0.92
361.0	64.8	0.029	48	5.55	3.70	0.06	0.50	0.10	0.92

Exchange: B, b1, A, a1, T, T0, S0 2.2 1.2 9.0 8.0 4.20 0.80 2.50 Gitter(s,x,y): 9 9 9

LtgsbdOffset: 0.50 Endiffmax 400. Fermien: 0.00

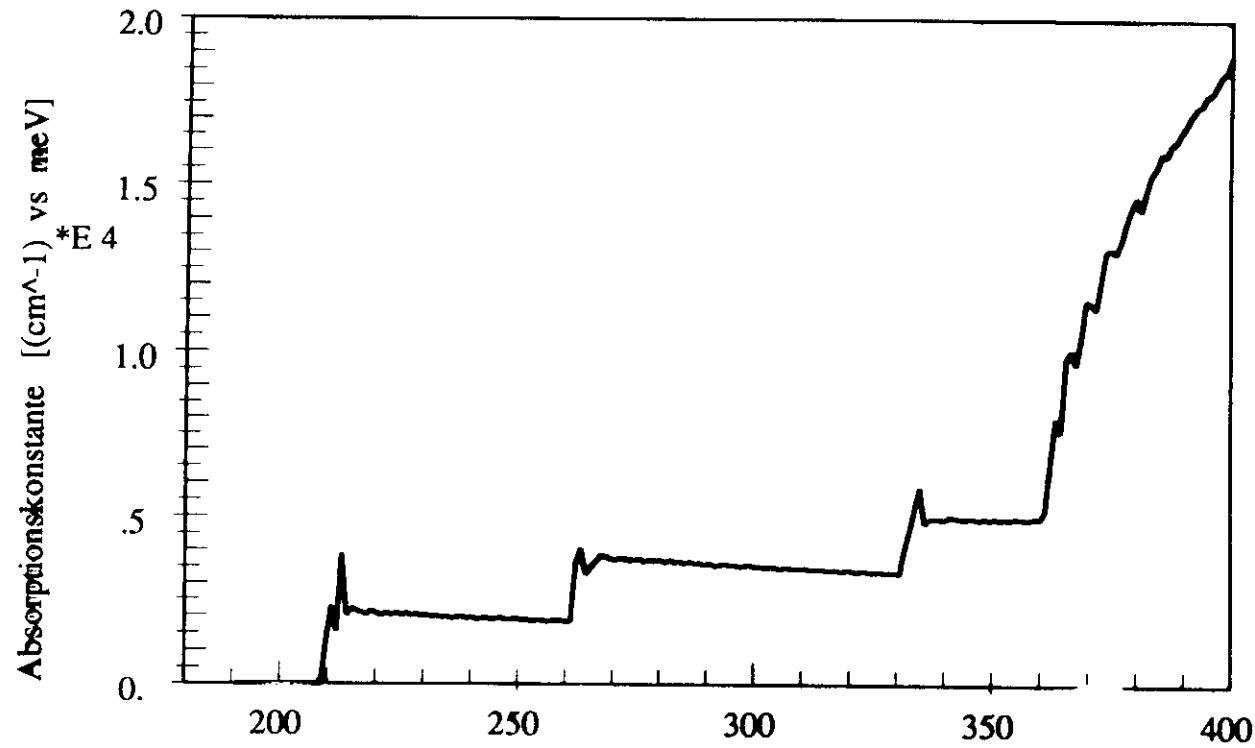

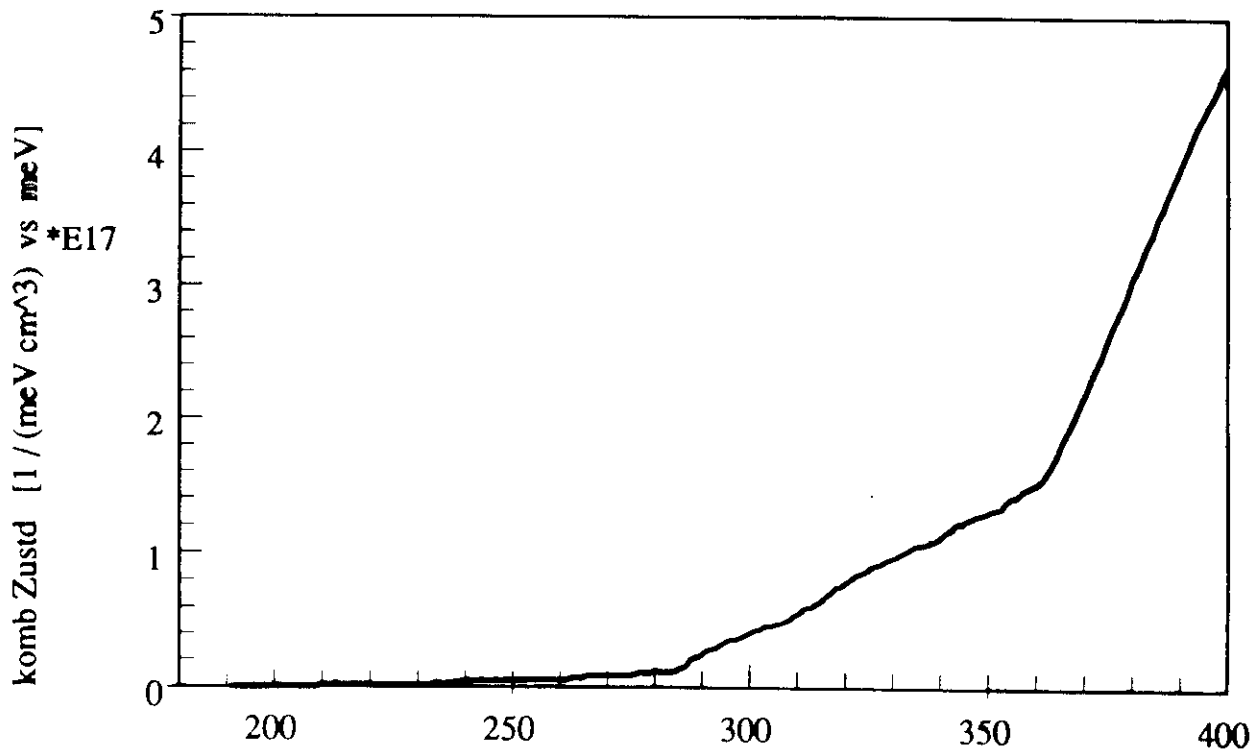

MQW148 5 STKL, Spline Fri Jul 16 19:01:10 1993 fileout: MQW14864a
WR 1 1 1 Tal 1 1 -1 epsinf 1.0

E_g	d	Konz	Stst	E_ps	Ps/Pp	mtc	mlc	mtv	mlv
189.7	9.3	0.000	7	6.02	3.42	0.06	0.50	0.10	0.92
361.0	64.8	0.029	27	5.55	3.70	0.06	0.50	0.10	0.92

Exchange: B, b1, A, a1, T, T0, S0 2.2 1.2 9.0 8.0 4.20 0.80 2.50 Gitter(s,x,y): 5 5 5
LtgsbdOffset: 0.50 Endiffmax 400. Fermien: 0.00

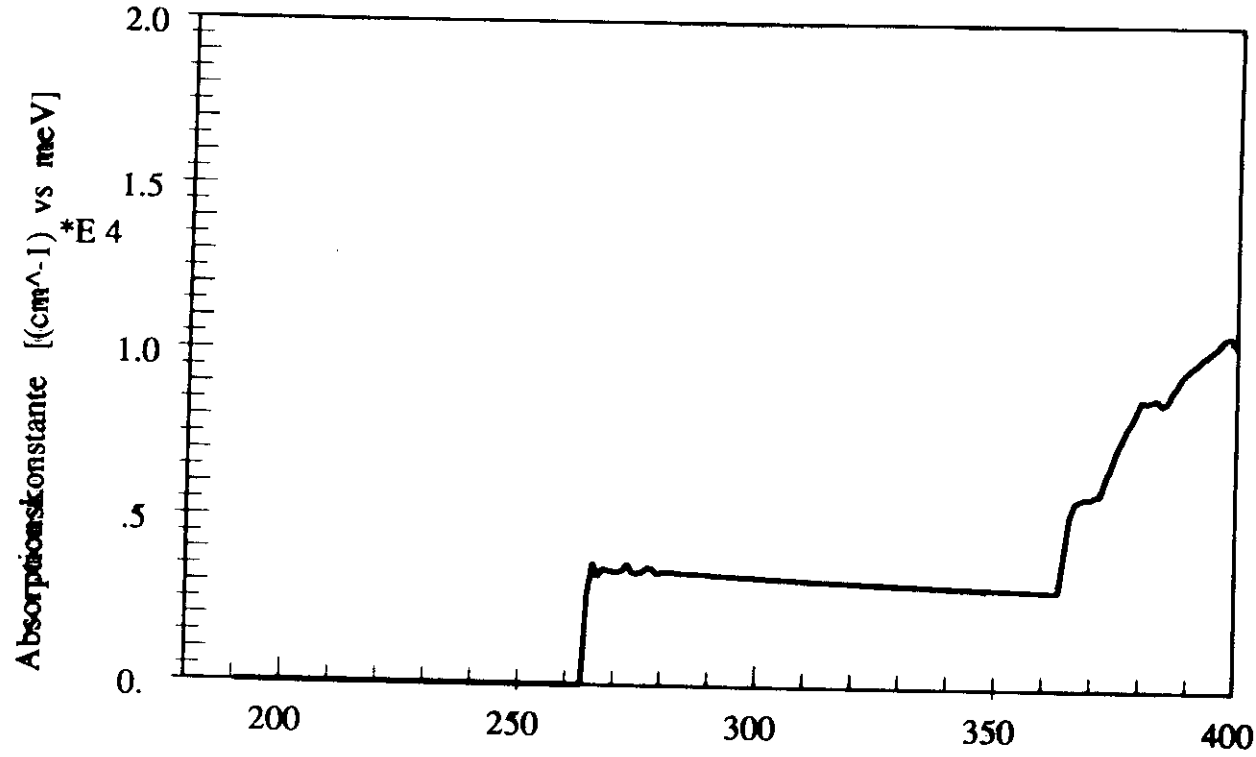

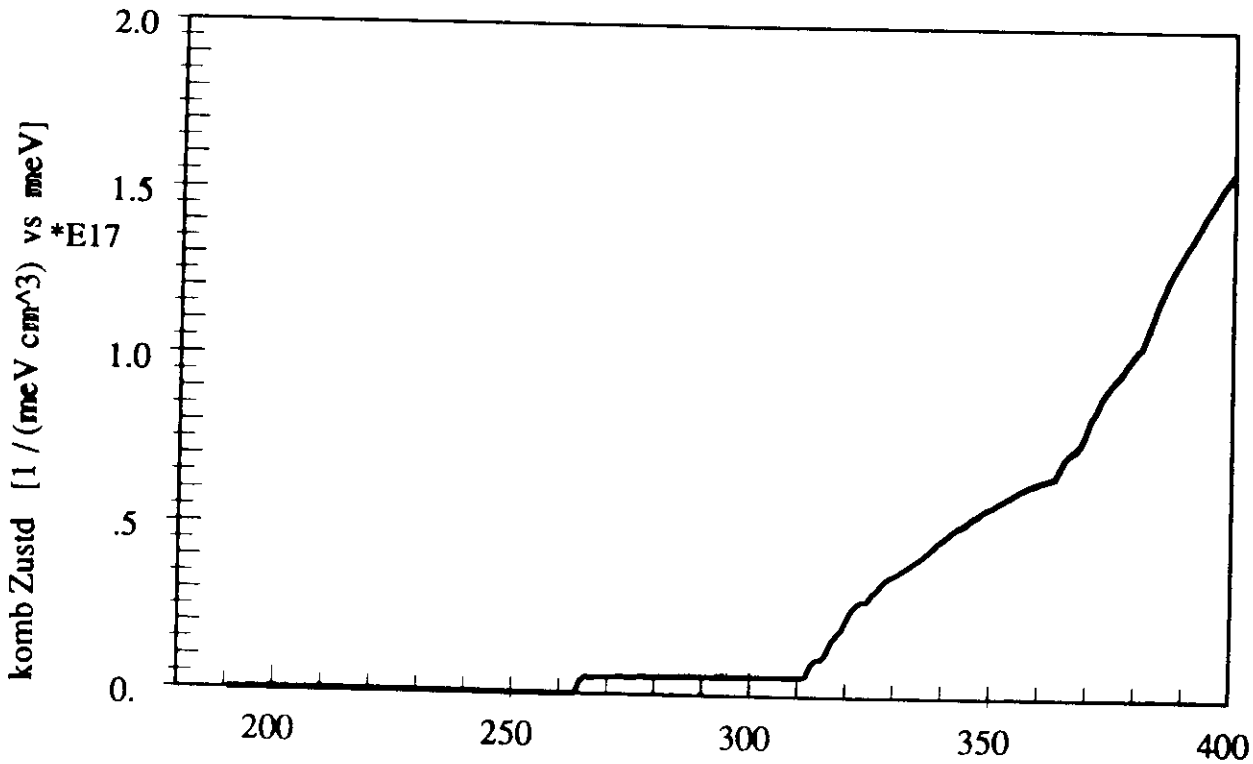

CALCULATION OF THE TRANSMISSION:

Transfer matrix method

(matching of the electromagnetic field at all interfaces):

$Pb_{1-x}Eu_xTe$: buffer, barrier layers:
essentially transparent

$\alpha^{PbEuTe}(\omega)$, $n^{PbEuTe}(\omega)$

PbTe: wells: absorption between confined states
$a(\omega)$, $n(\omega)$

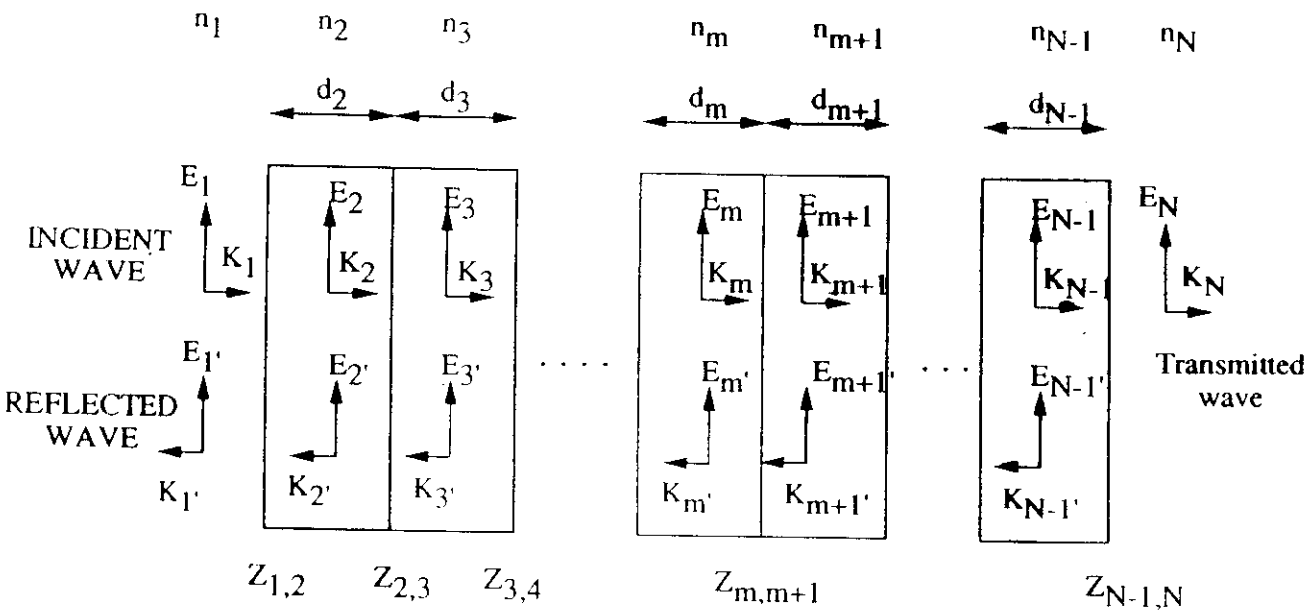

Transfer Matrix Method

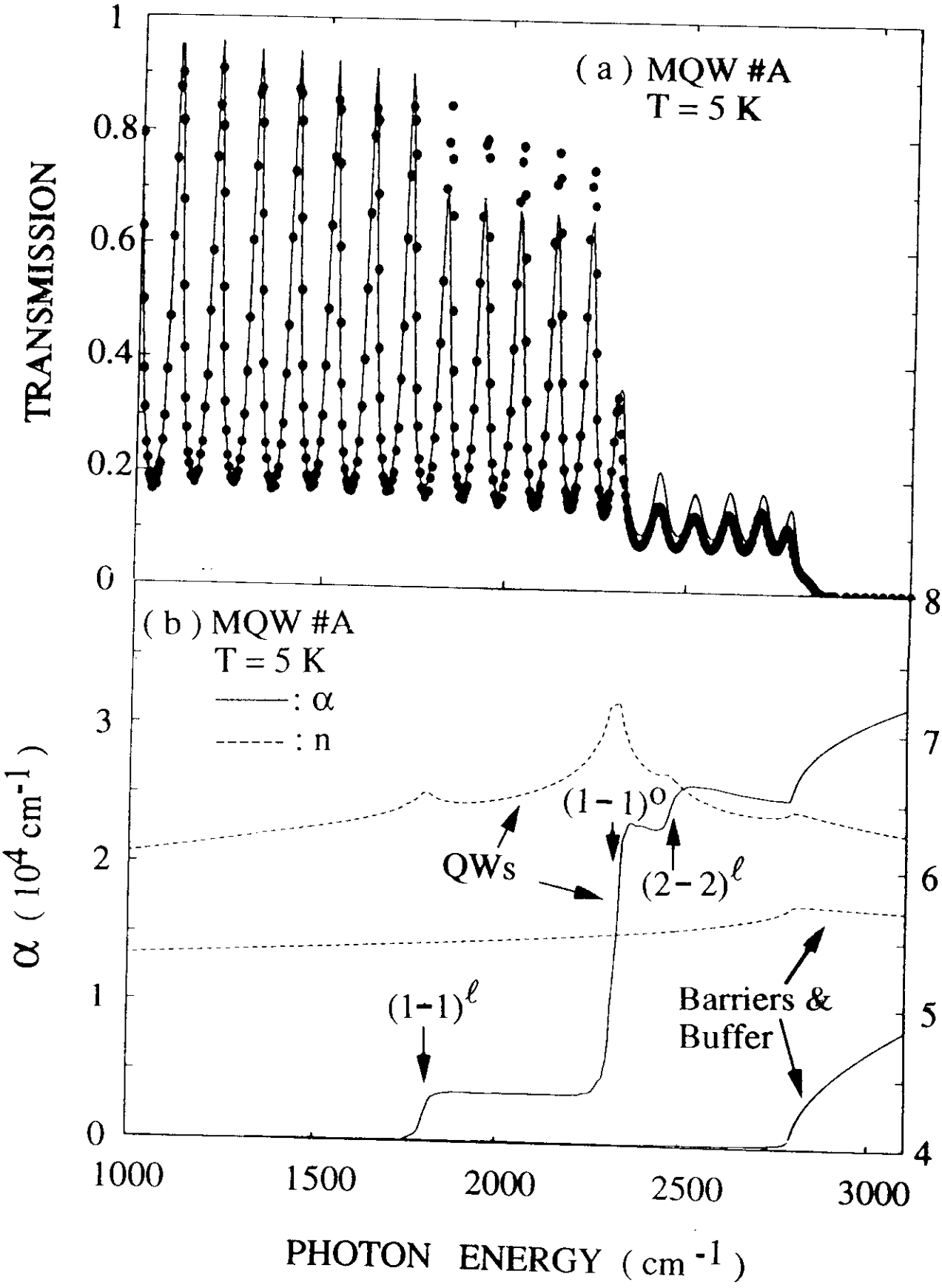
(a) MQW #A
T = 5 K
TRANSMISSION
1
0.8
0.6
0.4
0.2
0
(b) MQW #A
T = 5 K
——— : α
----- : n
α (10^4 cm^-1)
3
2
1
0
8
7
6
5
4
QWs
(1 – 1)^o
(2 – 2)^ℓ
(1–1)^ℓ
Barriers &
Buffer
1000
1500
2000
2500
3000
PHOTON ENERGY (cm^-1)

HL Übersteruktur & Magnetfeld

Voigt: $E \parallel B \perp Wr \parallel k$

$E \perp B$

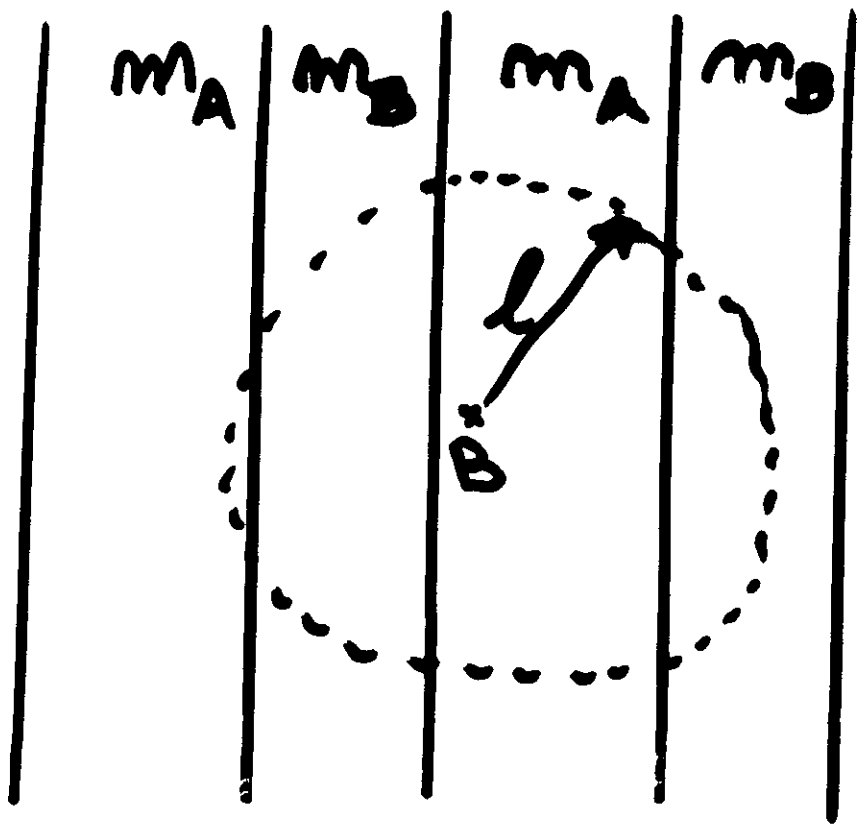

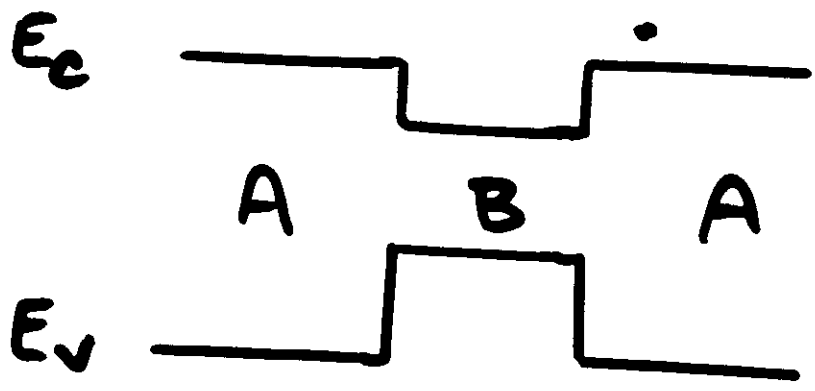

Gegenläufige Effekte:

In B E_c tiefer, in A $m_A > m_B$

$\hbar\omega_c = \frac{\hbar^2}{\ldots}$ $\hbar\omega_{cA} < \hbar\omega_{cB}$

Coherent Anti Stokes Raman Scattering

CARS

zur Bestimmung d. Landé faktors

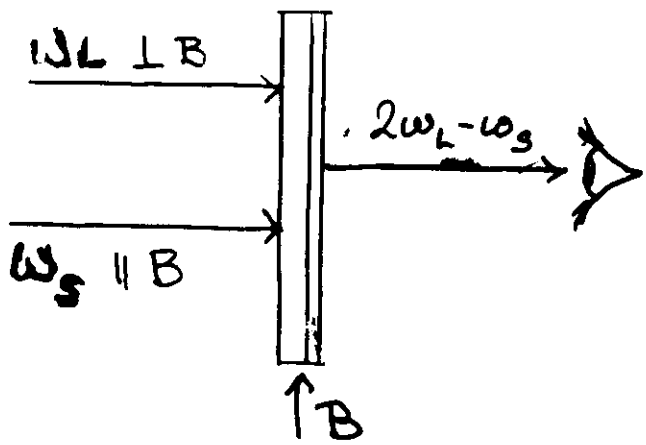

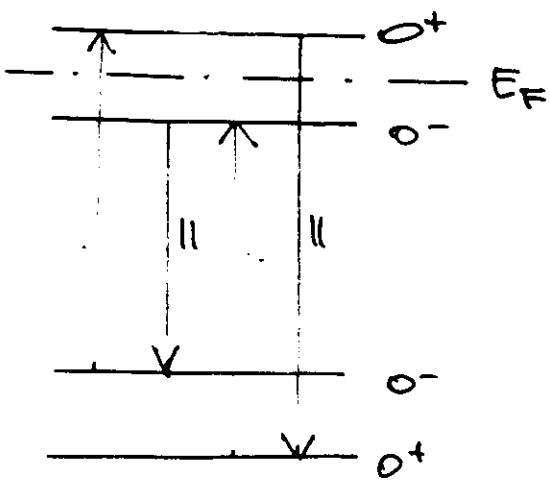

Maximum bei $2\omega_L - \omega_s$ für $\underline{\omega_L - \omega_s = g^* \mu_B B}$

CARS

$$I_{AS} = I_L^2 I_S L^2 |\chi|^2 \frac{9\omega_{AS}^2}{16c^4 n_{AS} n_L^2 n_S \epsilon_0^2} \times \left(\frac{\sin(\Delta k_{z_0} L/2)}{\Delta k_{z_0} L/2} \right)^2$$

$$\omega_{AS} = 2\omega_L - \omega_S$$

non linear susceptibility χ

$$\propto \frac{\langle d|P_{\parallel}|b\rangle^* \langle a|P_{\perp}|d\rangle \langle c|P_{\parallel}|a\rangle^* \langle b|P_{\perp}|c\rangle}{(\omega_{bd} - \omega_{AS} - i\Gamma_{bd})(\omega_{ba} - \omega_L + \omega_S - i\Gamma_{ba}) \cdot (\omega_{bc} - \omega_L - i\Gamma_{bc})}$$

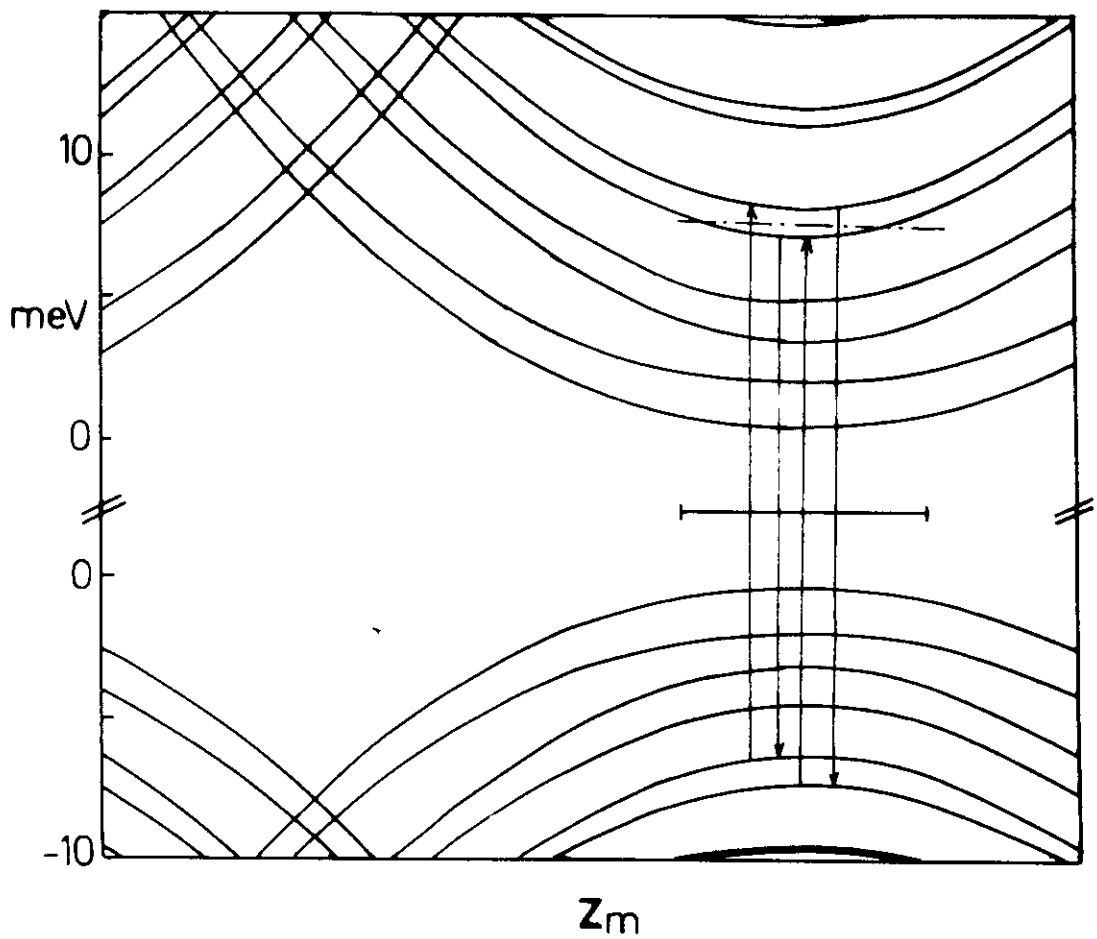
10
meV
0
0
-10
Zm

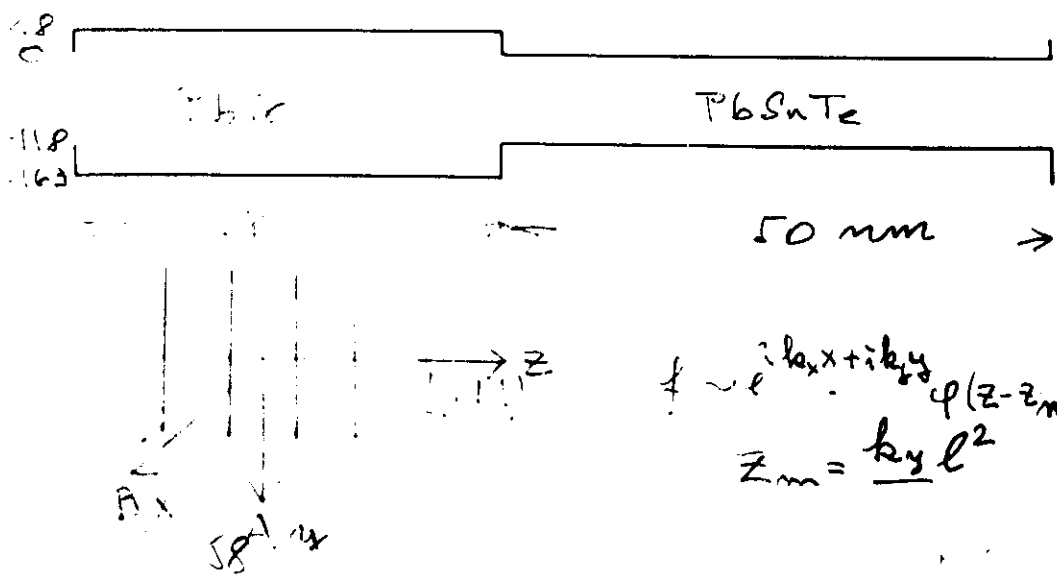
PbSnTe
50 nm
z
$\psi \sim e^{ik_x x + ik_y y} \varphi(z - z_m)$
$z_m = \frac{k_y l^2}{}$

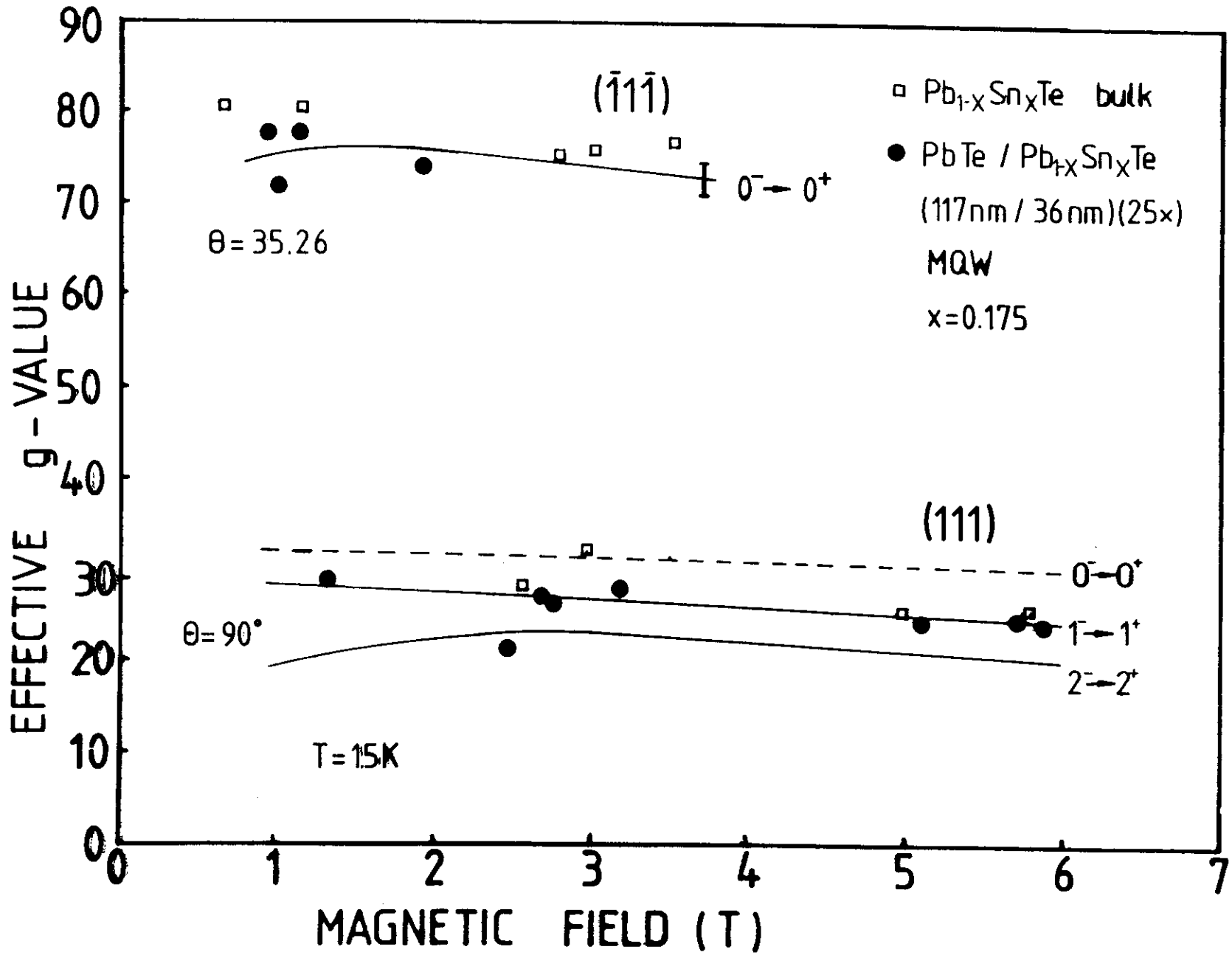
EFFECTIVE g-VALUE
MAGNETIC FIELD (T)
(1̄11̄)
□ Pb1-XSnXTe bulk
● PbTe / Pb1-XSnXTe
(117nm / 36nm)(25×)
MQW
x=0.175
θ= 35.26
0⁻ → 0⁺
(111)
θ= 90°
0⁻ → 0⁺
1⁻ → 1⁺
2⁻ → 2⁺
T = 1.5K

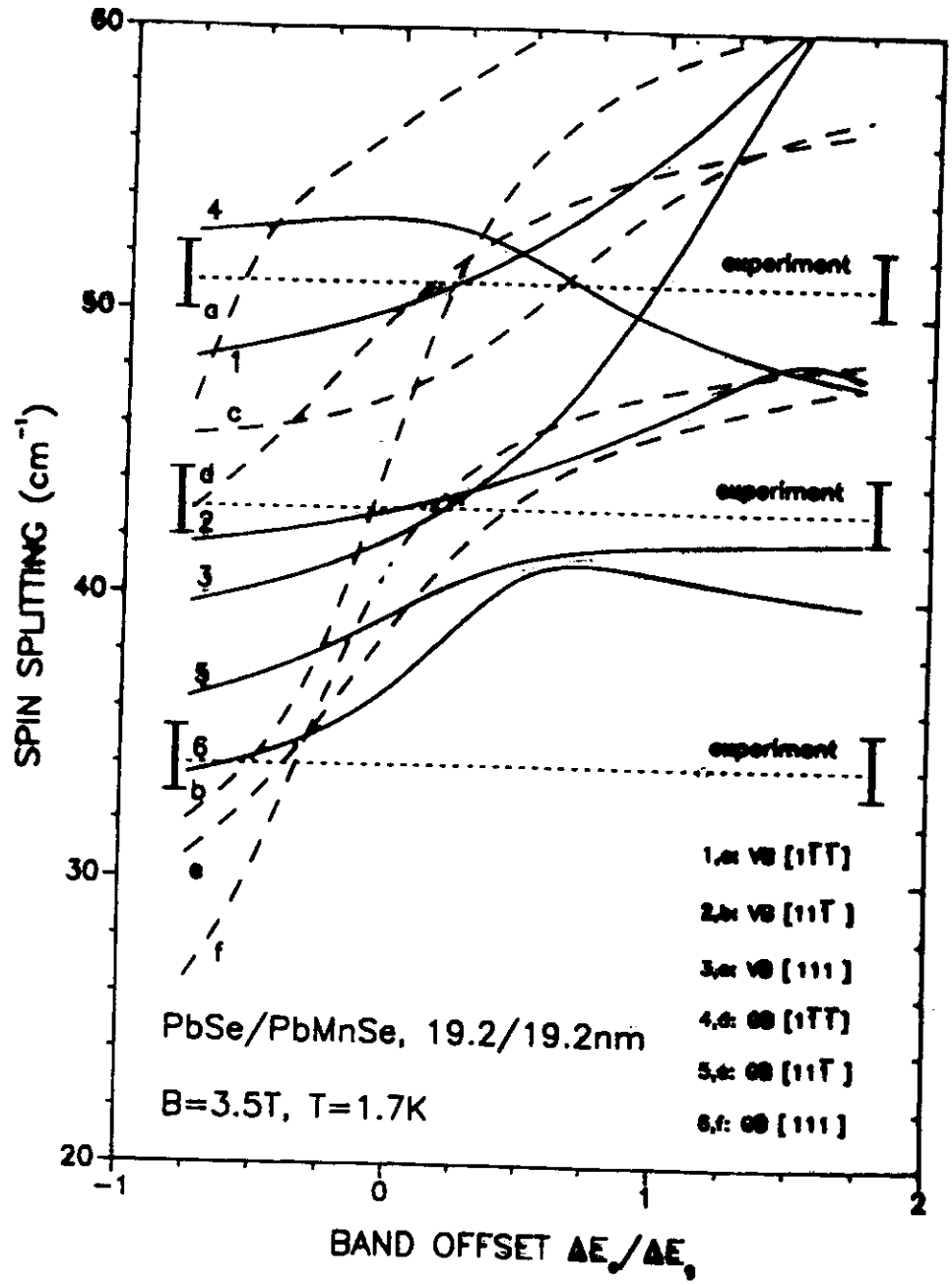
SPIN SPLITTING (cm⁻¹)
BAND OFFSET ΔE_c/ΔE_g
experiment
experiment
experiment
PbSe/PbMnSe, 19.2/19.2nm
B=3.5T, T=1.7K
60
50
40
30
20
−1
0
1
2

Ladungstraegerdichte Konturplot

PbMnSe58A Tue Apr 28 16:10:17 19Zeich 2- 7-92 11:33:44

Eg 146.3/ 203.3 D 13.0/ 13.0 WR 1 1 1 Tal 1 1-1 B 1 1 1 O-0.50 kB 0.0

Eps, Ps/Pp, mtlcvpm 3.6 3.8 1.4 1.4 0.3 0.9 0.3 0.4 0.3 0.9 0.3 0.4

gtlcvpm -4.0 -8.1 5.4 7.3 -6.8 -9.8 8.2 6.9

B= 3.5 E= 70.44 Niv 5 Stufen: 0.05

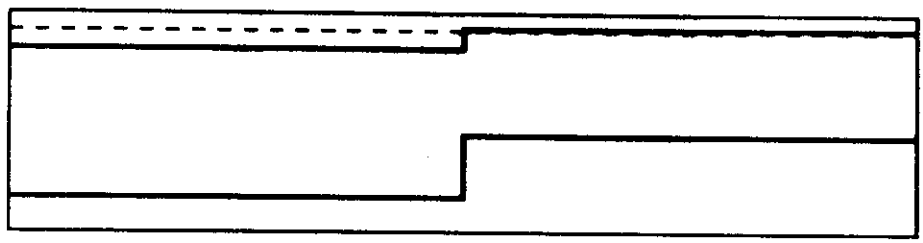

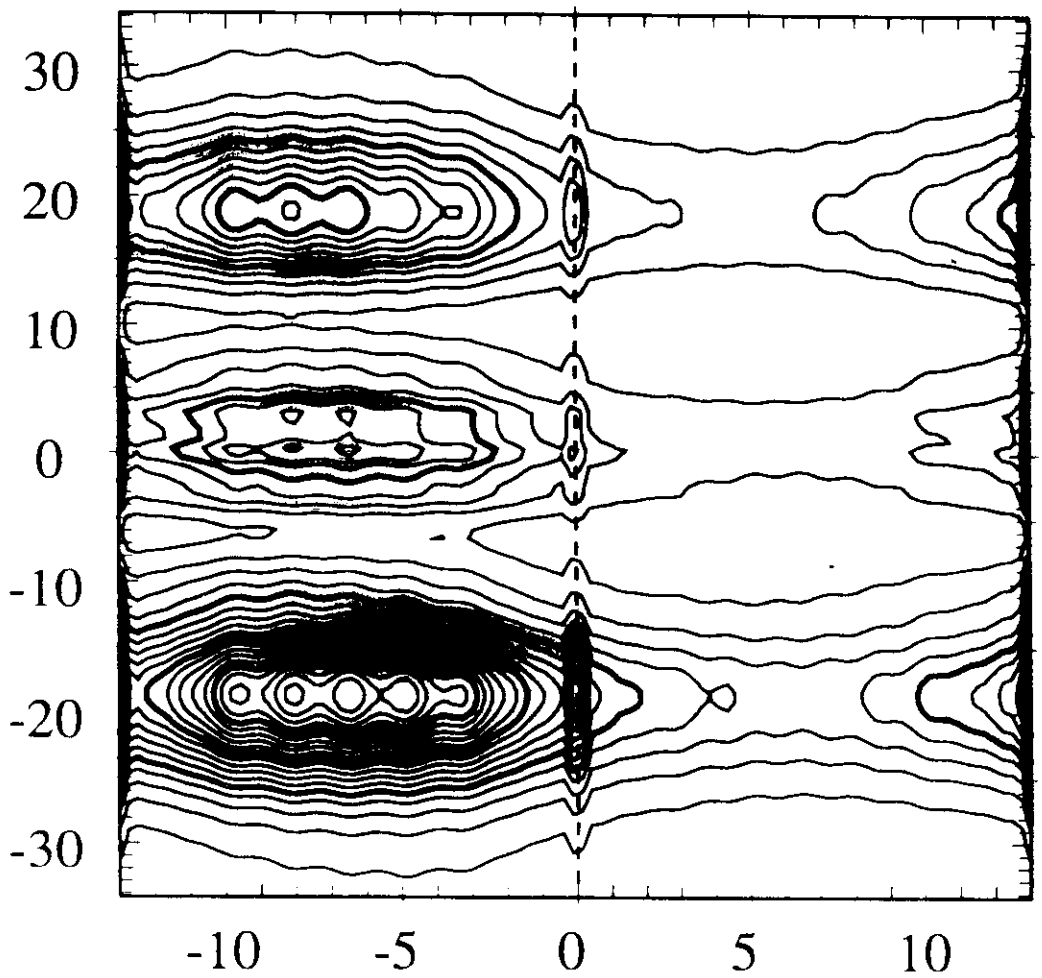

VERDÜNNTE MAGNETISCHE HALBLEITER

MAGNETISCHE FREMDIONEN

$Pb_{1-x}Mn_xTe$ $\quad$ $Pb_{1-x}Mn_xTe$

$x = 0.03$

Auf Pb Platz Mn^{++}

Mn^{++} $\quad 1s^2\ 2s^2 2p^6\ 3s^2 3p^6\ 3d^5\ 4s^2$

K L M

Hundsche Regel: (freies Atom)

$3d^5$: $L = 0$ voller antisymm. Raum

$S = 5/2$ voller symm. Spinzustand

$$\vec{B}_{ind} = \frac{2\mu_B}{\hbar c} \int d^3r' \rho(r') \nabla \times (S \times \nabla) \frac{1}{4\pi |r - r'|}$$

↑

Dichte d. magn. Momente

FRAGEN:

Ist Hundsche Regel im Kristall gültig?

(ist $S = 5/2$?) EPR ✓

Sind die Mn^{++} unabhängig
oder (anti-) ferr($\begin{smallmatrix}o\\i\end{smallmatrix}$) magnetisch geordnet

Experiment: paramagnetisch

Keine HOH atomaren Ionen:

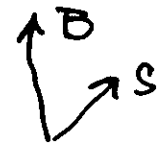

$$\langle S_B \rangle = - S B_S(z)$$ thermischer Mittelwert

$$z = \frac{g \mu_B S B}{k_B (T + T_0)}$$

$$B_S(z) = \frac{2S+1}{2S} \operatorname{cth}\left[\frac{2S+1}{2S} z\right] - \frac{1}{2S} \operatorname{cth} \frac{z}{2S}$$

$(g = 2,\ S = 5/2)$

Brillouinfunktion

Experimentelle Magnetisierungskurven
gefittet mit $S = 2.25$, $T_0 = 1.8\,K$
für $1.2 < T < 12\,K$

Wechselwirkung Mn^{++} – Valenzelektr.

a) Magnet. WW

$$H = -\mu \cdot B = -\mu_B \sigma \cdot B$$

$$H \approx \frac{5\mu_B \cdot 2\mu_B}{r^3} \approx \frac{1}{(137)^2}\left(\frac{a_0}{r}\right)^3 Ry$$

für $r \sim 2\text{Å}$: $H \sim 10^{-4}\,eV$

klein gegen elektrostat. Energie-differenzen ($\sim 0.1\,eV$)

b) Elektrostat. Austauschww.

zw. $3d^5$ u. Valenzelektronen

$$H = \sum_i (T_i + V_i) + \frac{1}{2}\sum_{i,j} \frac{e^2}{|r_i - r_j|}$$

eigentl. wellenantisymm (Pauli)

Elektronenaustauschwechselwirkung.

Pauliprinzip

$3d^5$ + Valenzel.

2 Möglichkeiten

$$\Sigma \equiv S + \sigma = \begin{cases} \frac{5}{2} + \frac{1}{2} & \text{symm. Spinanteil} \\ & \text{antisymm. Raumanteil} \\ & \text{Energie } E_+ \quad (: \text{Triplett}) \\ \frac{5}{2} - \frac{1}{2} & \text{komplizierte Spin- u. Raumsymmetrie} \\ & \text{Energie } E_- \quad (: \text{Singulett}) \end{cases}$$

↑ Gesamtspin

„äquivalenter Hamilton mit 2 Eigenwert

$$H = \frac{\Sigma^2 - 3\cdot(3+1)}{2(2+1) - 3\cdot(3+1)} E_- + \frac{\Sigma^2 - 2(2+1)}{3(3+1) - 2(2+1)} E_+$$

$$\Sigma^2 = S^2 + \sigma^2 + 2S\cdot\sigma$$

$$H_{\text{eredu}} = \text{const} - J\, S\cdot\sigma$$

PHOTOMAGNETIZATION

i) **CO-Laser 215 - 245 meV (circularly polarized)**

ii) **Excitation within PbTe wells.**

iii) **Light-induced magnetization in PbMnTe due to tails of electron wavefunctions from exeited spinpolarized carriers in diamagnetic PbTe-wells.**

iv) **Comparison with photoluminescence-spectra.**

v) **Polarity of photomagnetization in comparison to a "bulk" epilayer**

vi) **Saturation of photomagnetization**

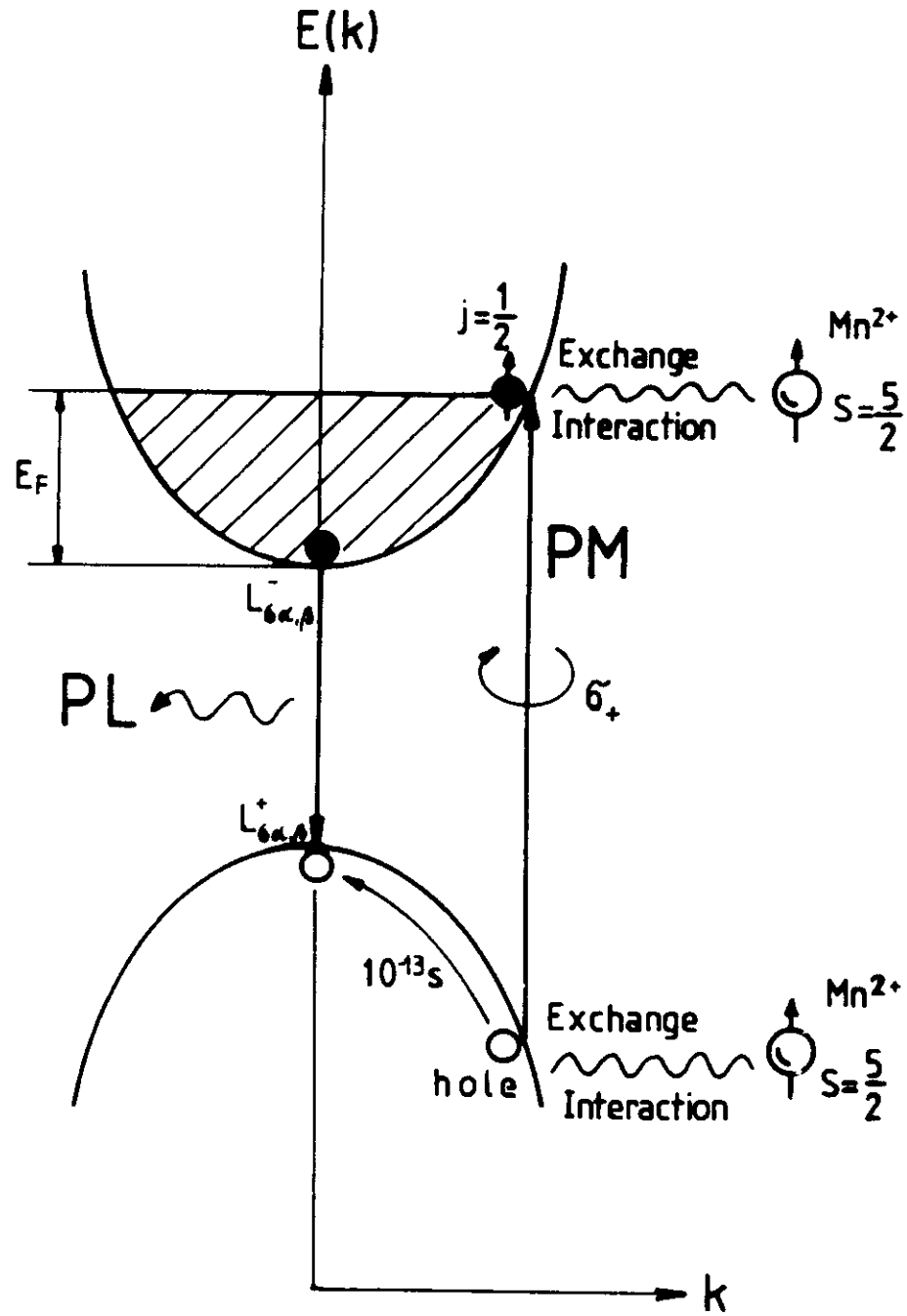
E(k)
j=1/2
Exchange
Interaction
Mn2+
S=5/2
EF
PM
L-6α,β
PL
6-
L+6α,β
10-13s
hole
Exchange
Interaction
Mn2+
S=5/2
k

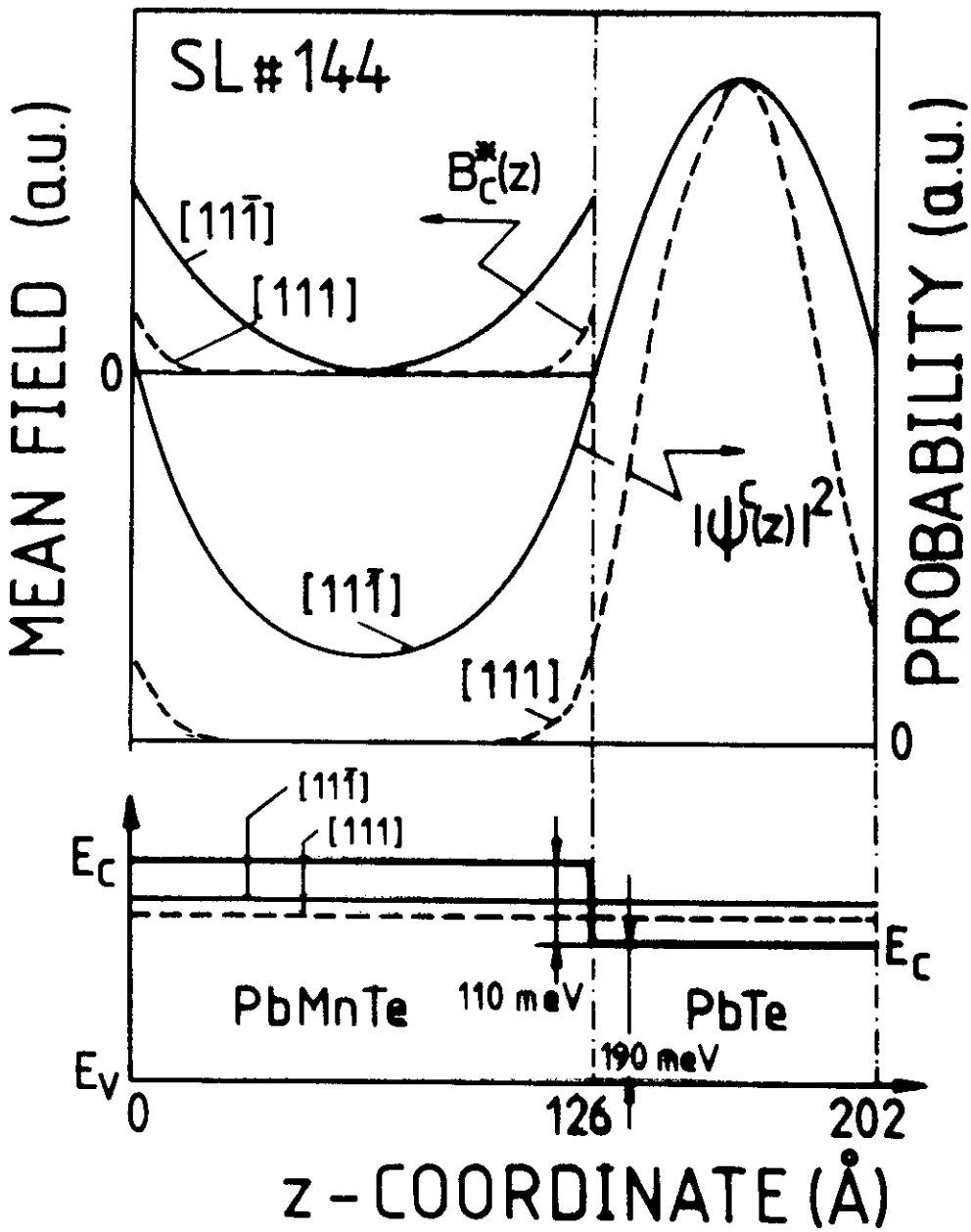
SL#144
MEAN FIELD (a.u.)
PROBABILITY (a.u.)
$B_C^*(z)$
[11$\bar{1}$]
[111]
0
$|\psi(z)|^2$
[11$\bar{1}$]
[111]
0
[11$\bar{1}$]
[111]
E_C
E_C
PbMnTe
110 meV
PbTe
190 meV
E_V
0
126
202
z - COORDINATE (Å)

SL#114

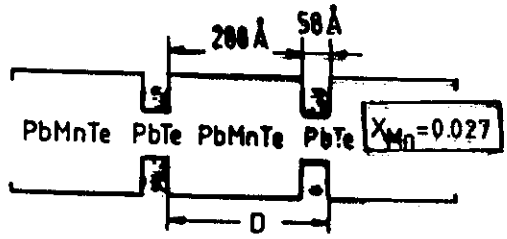
200 Å
50 Å
PbMnTe
PbTe
PbMnTe
PbTe
X_{Mn}=0.027
D

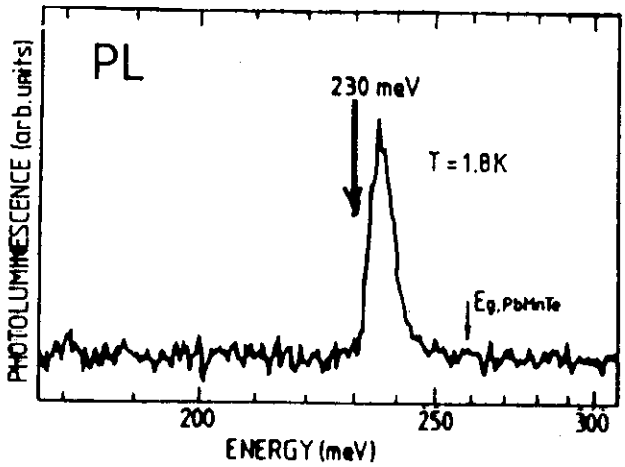
PL
230 meV
T = 1.8K
$E_{g,PbMnTe}$
PHOTOLUMINESCENCE (arb. units)
200
250
300
ENERGY (meV)

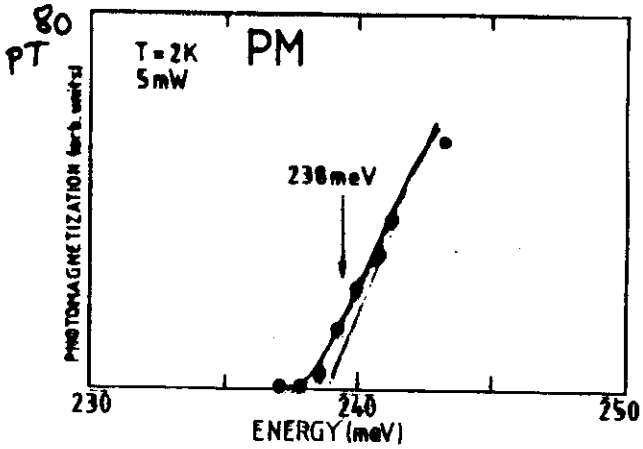
80
PT
T = 2K
5mW
PM
238meV
PHOTOMAGNETIZATION (arb. units)
230
240
250
ENERGY (meV)

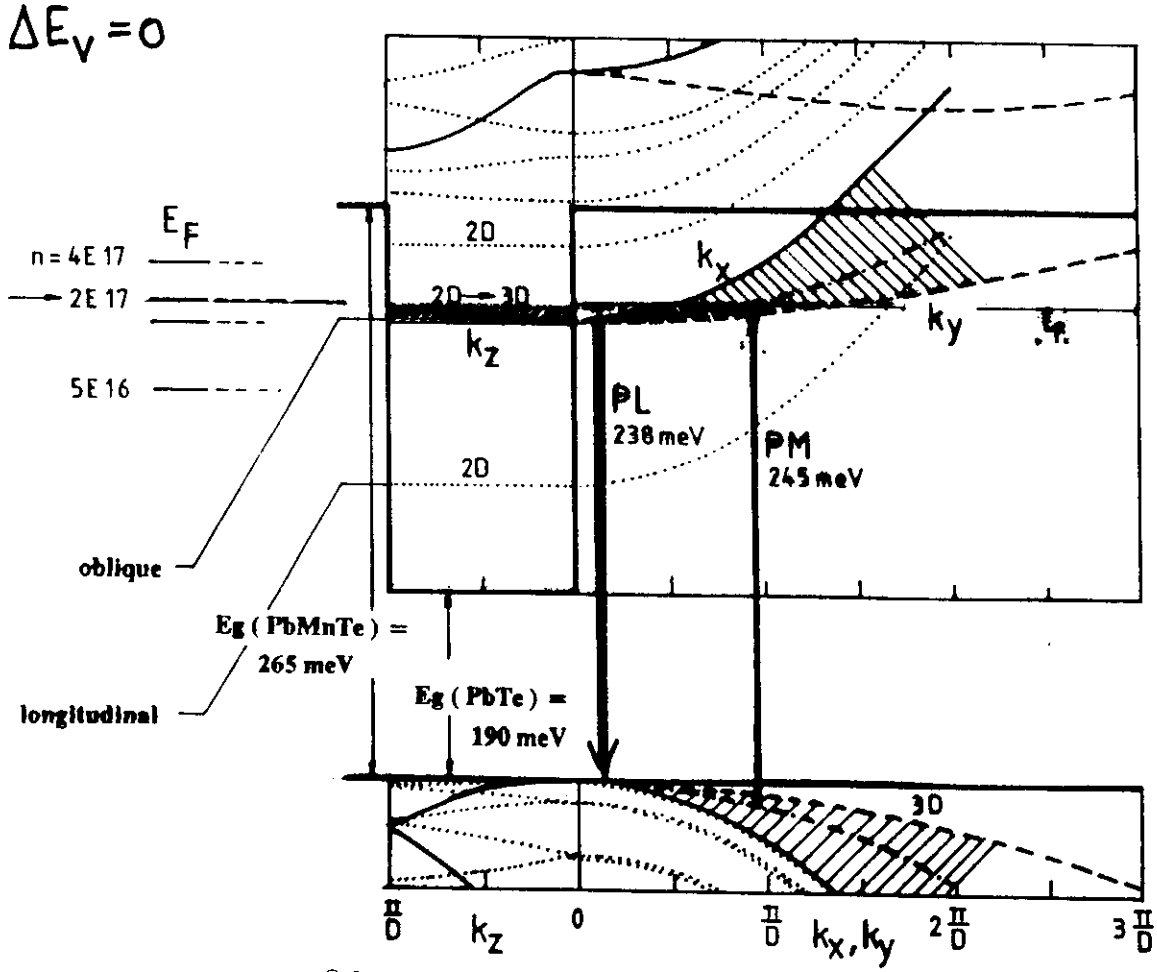
$\Delta E_V = 0$
E_F
n = 4E 17
2E 17
5E 16
2D
2D → 3D
k_x
k_y
k_z
PL
238 meV
PM
245 meV
2D
oblique
Eg (PbMnTe) =
265 meV
longitudinal
Eg (PbTe) =
190 meV
3D
$\frac{\pi}{D}$
k_z
0
$\frac{\pi}{D}$
k_x, k_y
$2\frac{\pi}{D}$
$3\frac{\pi}{D}$

THEORY:

PHOTOEXCITATION GENERATES

KRAMERS SPIN POLARIZED CARRIERS; CAUSE VIA s-d EXCHANGE INTERACTION A POLARIZATION OF THE

Mn^{2+} ($S = 5/2$) d -ELECTRONS

PHOTOMAGNETIZATION

(MAGNETIC MOMENT OF SPIN POLARIZED VALENCE AND CONDUCTION ELECTRONS IS NEGLIGIBLE COMPARED TO MAGNETIC MOMENT M OF SPIN POARIZED Mn^{2+} (S))

$$M = g\mu_B \langle S_z \rangle \frac{x}{\Omega} \frac{d_{Mn}}{d_{Mn}+d_{Pb}}$$

density of Mn-ions

Ω: volume of Wigner-Seitz-cell

$B = \mu_0 M$

CALCULATION OF STEADY STATE ρ:

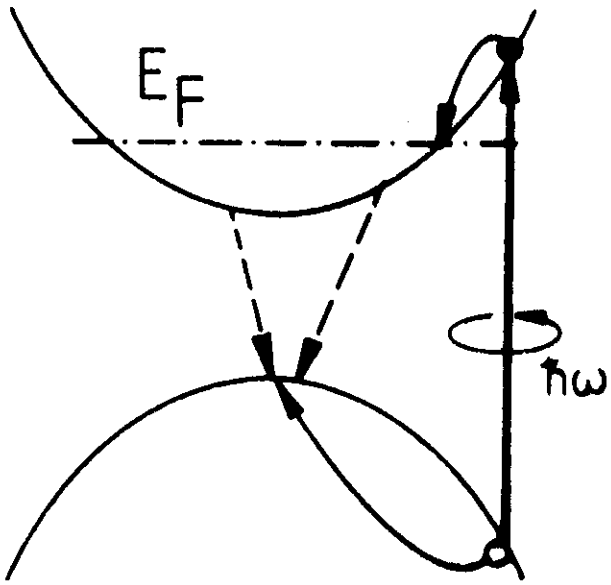

n-type samples:

HOLE POLARIZATION VANISHES QUICKLY. RESULTING POLARIZATION IN CB DUE TO GENERATED ELECTRONS.

RATE EQUATIONS:

$$\frac{\partial \rho^{\pm}}{\partial t} I_{gen} = \frac{\partial \rho^{\pm}}{\partial t} I_{Rec} + \frac{\partial \rho^{\pm}}{\partial t} I_{SF}$$

$$\frac{\partial \rho^{\pm}}{\partial t} I_{Rec} = \frac{\rho^{\pm}}{\tau_R} \quad ; \quad \frac{\partial \rho^{\pm}}{\partial t} I_{SF} = \pm \frac{\rho^{+} - \rho^{-}}{\tau_{SF}}$$

$$\rho^{+} - \rho^{-} = \frac{\tau_R \, \tau_{SF}}{\tau_{SF} + 2\tau_R} \left(\frac{\partial \rho^{+}}{\partial t} I_{gen} - \frac{\partial \rho^{-}}{\partial t} I_{gen} \right)$$

CALCULATION OF ENERGY DISPERSION

WAVE FUNCTIONS AND GENERATION RATE WITH ENVELOPE FUNCTION APPROXIMATION

$$H = \begin{pmatrix} E_v - \frac{h^2k_\perp^2}{2m_t^+} - \frac{h^2k_z^2}{2m_l^+} & P_{\parallel}k_3\sigma_3 + P_\perp(k_1\sigma_1 + k_2\sigma_2) \\ hc & E_c + \frac{h^2k_\perp^2}{2m_t^-} + \frac{h^2k_z^2}{2m_l^-} \end{pmatrix}$$

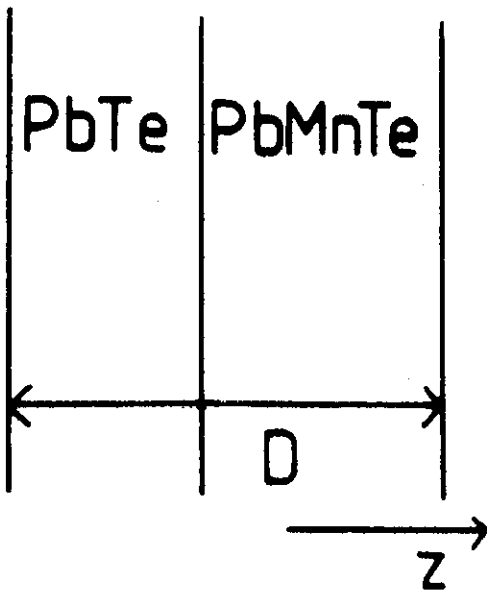

z-dependent parameters:

$E_c(z)$, $E_v(z)$
$P_{\parallel}$, $P_\perp(z)$
$m_l^{\pm}$, $m_t^{\pm}(z)$

$Hf_k = E_k f_k$ (hermitized Hamiltionian)

with $f_b(z+D) = \exp(ik_zD)\, f_b(z)$

$\vec{k} = (k_x, k_y, k_z)$ (k_x, k_y: in plane momenta)

AVERAGE SPIN $\langle S_z \rangle$ GIVEN BY

$$\langle S_z \rangle = \frac{\sum_{j=-S}^{S} j \exp(-jb_z/k_BT)}{\sum_{j=-S}^{S} \exp(-jb_z/k_BT)}$$

$$= -\left(S+\frac{1}{2}\right) \mathrm{ctgh}\left(S+\frac{1}{2}\right) b_z/k_BT + \frac{1}{2} \mathrm{ctgh}\, \frac{1}{2}\, b_z/k_BT$$

where

$$\vec{b} = \frac{\Omega}{(2\pi)^3} \int \mathrm{Tr}\, \rho_{\vec{k}} \frac{\partial}{\partial \vec{s}} H_{exch}\, \vec{k}\, d^3k$$

(proportional to mean molecular field)

Tr extends over the Kramers pair

H_{exch} =

$$\begin{pmatrix} A\sigma_zS_z+a_1(\sigma_xS_x+\sigma_yS_y) & 0 \\ 0 & B\sigma_zS_z-b_1(\sigma_xS_x+\sigma_yS_y) \end{pmatrix}$$

numerical values:
A=-182 meV, a_1=-288meV; B=-33meV, b_1=27meV

GENERATION RATE:

$$\dot{\rho}_{\vec{k}\,\alpha,\beta} = \sum_i \langle \alpha\vec{k} | \pi^+ | i\vec{k} \rangle \langle \beta\vec{k} | \pi^+ | i\vec{k} \rangle^*$$

$$\times\ \delta\left(E(\vec{k}) - E_i(\vec{k}) - h\omega\right)\left(1 - f_{\alpha,\beta}\right) f_i$$

$$H^{\alpha,\beta}_{exch,\vec{k}} = \langle \alpha,\vec{k} | H_{exch} | \beta,\vec{k} \rangle \ ;\ \alpha = \pm,\ \beta = \pm$$

For $b_z << k_B T$

$$\langle S_z \rangle = - \frac{b_z}{3k_B T}\ S\left(S + \frac{1}{2}\right)$$

MOLECULAR FIELDS

Def.:

$$\langle \hat{H}_{exch} \rangle = -g\,\mu_B\,\vec{S}\cdot\vec{B}^{*}$$ (per carrier)

$\vec{S}$ — average Mn-Spin

EXPECTATION VALUE

$$\frac{\int d\vec{k}\cdot \mathrm{Trace}\left[\hat{\rho}^{\pi^+}(\vec{k})\,\hat{H}_{exch}\right]}{\int d\vec{k}\cdot \mathrm{Trace}\left[\hat{\rho}^{\pi^+}(\vec{k})\right]}$$

Interband-Transition Density Matrix for π^+-Polarization

$$\rho^{\pi^+}_{\alpha\beta}(k) = \sum_i \langle k,\alpha|\pi^+|i\rangle\langle k,\beta|\pi^+|i\rangle^{*}$$

i — initial, f — final } state

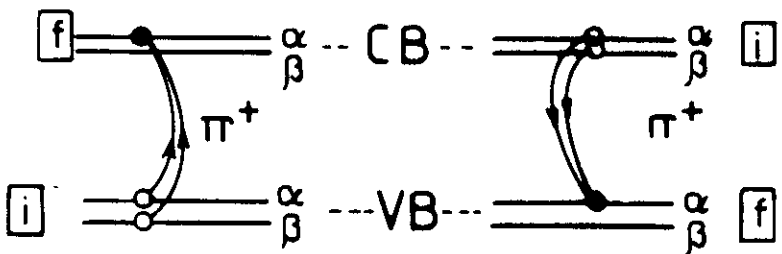

$\rho^{C}_{\alpha\alpha}$ $\rho^{V}_{\alpha\alpha}$

$$\vec{B}^{*}_{C,V} = -\frac{1}{g\,\mu_B}\frac{\partial}{\partial \vec{S}}\int d\vec{k}\cdot \mathrm{Trace}\left[\hat{\rho}^{\pi^+}\hat{H}_{exch}\right]$$